Journal of Sound and Vibration 330 (2011) 1166–1195

Contents lists available at ScienceDirect

Journal of Sound and Vibration

journal homepage: www.elsevier.com/locate/jsvi

On the acoustic modes in a duct containing a parabolic shear flow

L.M.B.C. Campos *, J.M.G.S. Oliveira

Centro de Ciências e Tecnologias Aeronauticas e Espaciais (CCTAE), and Área Científica de Mecânica Aplicada e Aeroespacial (ACMAA), Instituto Superior Técnico, 1049-001 Lisboa, Portugal

ARTICLE INFO

Article history:
Received 15 January 2009
Received in revised form
13 July 2010
Accepted 22 September 2010
Handling Editor: Y. Auregan
Available online 9 November 2010

ABSTRACT

The exact solution of the acoustic wave equation in an unidirectional shear flow with a parabolic velocity profile is obtained, representing sound propagation in a plane, parallel walled duct, with two boundary layers over rigid or impedance walls. It is shown that there are four cases, depending on the critical level(s) where the Doppler shifted frequency vanishes: (i) for propagation upstream the critical levels are outside the duct (case II); (ii) for propagation downstream there may be two (case IV), one (case I) or no (case III) critical level inside the duct. The acoustic wave equation is transformed in each of the four cases to particular forms of the extended hypergeometric equation, which has power series solutions, some involving logarithmic singularities. In the cases where critical levels occur, at real or 'imaginary' distance, matching of two or three pairs of solutions, valid over regions each overlapping the next, is needed. The particular case of the parabolic velocity profile is used to address general properties of sound in unidirectional shear flows. For example, it is shown that for ducted shear flows, there exist a pair of even and odd eigenfunctions, in the absence of critical levels. It is also proved, in more than one instance, that there is no single set of eigenvalues and eigenfunctions valid across one or two shear layers. This leads to the general conjecture, considering the acoustics of shear flows in ducts, that critical levels separate regions with distinct sets of eigenvalues and eigenfunctions.

1. Introduction

The propagation of sound in shear flows is a major research area in aeroacoustics [1–10], relevant to the acoustics of (i) shear flows and shear layers of jets [11–20]; (ii) boundary layer over walls [21–28]; (iii) duct and nozzles, including liners and bends [29–52]. In the wake of turbines the flow may have swirl as well as shear [8,53–66]. The real shear layers, boundary layers and wakes are often turbulent [67–71], leading to other acoustic phenomena, like spectral and directional broadening [72–75].The common occurrence of turbulent shear flows is ascribed to the instabilities of laminar shear flows: the latter are described by the same equations as for sound propagation, except that the frequency is taken to be real for sound waves, and complex for instability waves. Although the acoustic wave equation in a unidirectional shear flow has been known for some time [76–78], there are few exact solutions in the literature [79,66]. The simplest case of sound of in a mean flow with a linear shear velocity profile, has been solved in terms of: (i) parabolic cylinder functions [80]; (ii) Whittaker functions [81,82]; (iii) confluent hypergeometric functions [83–85]; (iv) eigenfunctions even and odd relative to the critical layer, which always exists for a linear shear flow [86]. The linear velocity profile has also been considered for isentropic non-homentropic flow, implying the presence of temperature gradients [87]. A source has been considered outside an isothermal [81] and

* Corresponding author. Tel.: +351 218417267; fax: +351 218417539.
E-mail address: lmbcampos.aero@mail.ist.utl.pt (L.M.B.C. Campos).

0022-460X/$ - see front matter © 2010 Elsevier Ltd. All rights reserved.
doi:10.1016/j.jsv.2010.09.021

non-isothermal [88] shear flow. The linear shear velocity profile may be matched to uniform stream(s), to form boundary layer and shear velocity profiles; the latter have 'kinks' at the junctions, corresponding to jumps of mean flow vorticity, which may be unstable. Exact solutions of the acoustic wave equation in an unidirectional sheared mean flow with a smooth velocity profile, hence continuous mean flow vorticity, have been obtained for: (i) the exponential velocity profile [89] representing a boundary layer; (ii) the hyperbolic tangent velocity profile [90] representing a shear layer. The present paper gives the exact solution for a parabolic velocity profile, including the two wall boundary layers in a plane, parallel walled duct.

The preceding solutions concern the linear, non-dissipative acoustic wave equation, and thus exclude viscosity [91], whose effects on sound attenuation are comparable to thermal conduction [92] and relaxation [93]. Thus the sound propagation in an exponential shear flow is not a perturbation of the asymptotic suction profile [94] and the sound propagation in a parabolic shear flow is not a perturbation of Poiseuille flow. An important feature in the acoustics of shear flows, is the occurrence of critical levels where the Doppler shifted frequency vanishes, corresponding to singularities of the wave equation. Critical levels occur for a variety of waves in fluids [95–98], e.g. gravity [99], inertial [100], instability [101,102] and hydromagnetic [103,104]. Critical levels also occur for atmospheric waves in the presence of dissipation, by viscosity [105,106], thermal conduction [107–109], thermal radiation [110], and electrical resistance [111] as well as mean flow [112]. The occurrence of critical levels, would separate the flow in regions with distinct sets of eigenvalues and eigenfunctions, if Klein's theorem did apply [113]; however, although the acoustic wave equation in an unidirectional shear flow can be put in a self-adjoint form, neither the Klein nor the Sturm–Liouville theorems apply, because the wavenumber appears not only in the 'eigenvalues' but also in other terms of the differential equation. Thus such useful theorems as the orthogonality and completeness of eigenfunctions, the number and spacing of their roots, the existence of eigenvalues and their asymptotic estimates, cannot be taken for granted. A second aim for the present paper is to use the exact solution of the acoustic wave equation in a shear flow with a parabolic velocity profile to investigate the general properties of sound in shear flows, leading to some: (i) counter-proofs, e.g. there can be no single set of eigenvalues and eigenfunctions in across a critical level; (ii) conjectures, e.g. critical levels separate regions of the flow with independent sets of eigenvalues and eigenfunctions.

Thus the present paper pursues (Section 1) two interwoven lines of research: (i) to obtain the exact solution of the acoustic wave equation in a parabolic shear flow, representing sound propagation in a duct with boundary layer over rigid or impedance walls (Section 2); (ii) to use these solutions to investigate general properties, like the occurrence of critical levels, and its implications, e.g. concerning the eigenvalues and eigenfunctions for the sound field (Section 3). The consideration of the critical levels of sound in a parabolic shear flow, leads (Section 3) to four cases: (I) the simplest case I is a critical level on the axis of the duct (Section 4), for which the whole flow region is covered by convergent power series of even and odd eigenfunctions, whose linear combination specifies the general wave field; (II) for sound propagation upstream, i.e. opposite to the mean flow, the critical levels lie outside the duct, and power series solutions around the axis still cover the whole flow region, although (Section 5) the differential equation to be solved is less simple, viz. of the extended [114,115] hypergeometric [116–118] type; (III) in the case III of downstream propagation such that the Doppler shifted frequency does not vanish in the flow region, there are critical levels at imaginary distance, which limit the radius of convergence of one pair of solutions of the wave equation, so that (Section 6) matching to another pair of solutions is needed; (IV) the final case IV, in which the Doppler shifted frequency vanishes in the flow region, involves two critical levels at which the sound field may have logarithmic singularities (Appendix A) and needs the matching of three pairs of solutions of the wave equation (Section 7), valid in three regions, each overlapping the next. It is possible to prove that, in the cases where one (Section 8) or two (Appendix B) critical levels occur, there is no single set of eigenvalues and eigenfunctions valid in the whole flow region. This leads to the following conjecture: the critical levels of sound in a shear flow separate regions with distinct sets of eigenvalues and eigenfunctions (Figs. 24 and 25). This corresponds to Klein's theorem [113], although the acoustic wave equation in a unidirectional shear flow (Fig. 1), put in self-adjoint form (Section 8), does not satisfy the conditions of Sturm–Liouville theory because the wavenumber appears not only in the 'eigenvalue' but also elsewhere. The plots of eigenfunctions in various cases (Figs. 4–15), show that they do not have the number of modes predicted by Sturmian theory for the corresponding eigenvalues (Figs. 2 and 3).

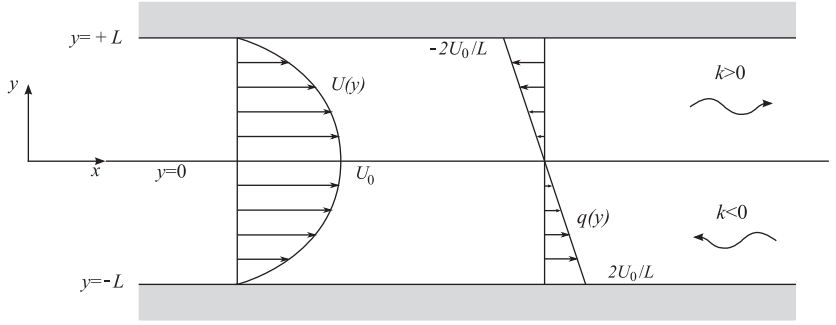

Fig. 1. Sound wave of frequency ω, and longitudinal wavenumber k, corresponding to horizontal wavevector parallel $k>0$ or anti-parallel $k<0$, to a parabolic shear flow, with velocity U_0 on the axis, and zero at the walls $y=\pm L$. The problem is to determine the eigenvalues k_n, and the corresponding eigenfunctions, for the even $E_n(y)$ and odd $F_n(y)$ modes of the acoustic pressure $P(y)$.

2. Acoustic wave equation and boundary conditions in a duct with a shear flow

The linearized, two-dimensional momentum (1) and continuity (2) equations read as

$$\frac{\mathrm{d}u}{\mathrm{d}t}+U'v+\frac{1}{\rho_0}\frac{\partial p}{\partial x}=0, \tag{1a}$$

$$\frac{\mathrm{d}v}{\mathrm{d}t}+\frac{1}{\rho_0}\frac{\partial p}{\partial y}=0, \tag{1b}$$

$$\frac{1}{c^2}\frac{\mathrm{d}p}{\mathrm{d}t}+\rho_0\left(\frac{\partial u}{\partial x}+\frac{\partial v}{\partial y}\right)=0, \tag{2}$$

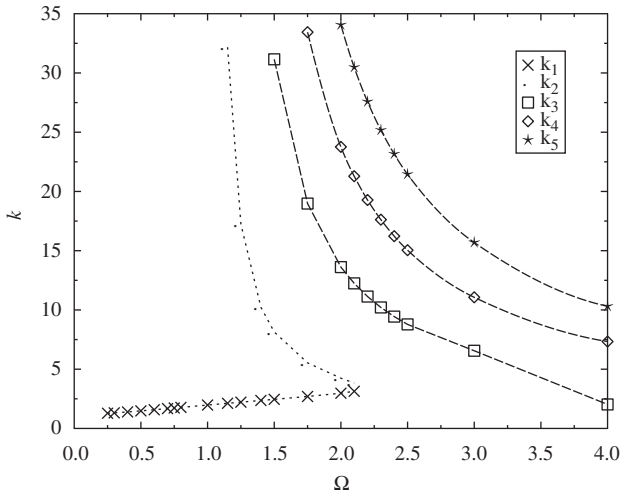

Fig. 2. First K_1 and second K_2 eigenvalue, as a function of dimensionless frequency Ω, for even mode $E_{1,2}$, in the case I of horizontal wavevector parallel to the mean flow velocity with critical level on the duct axis.

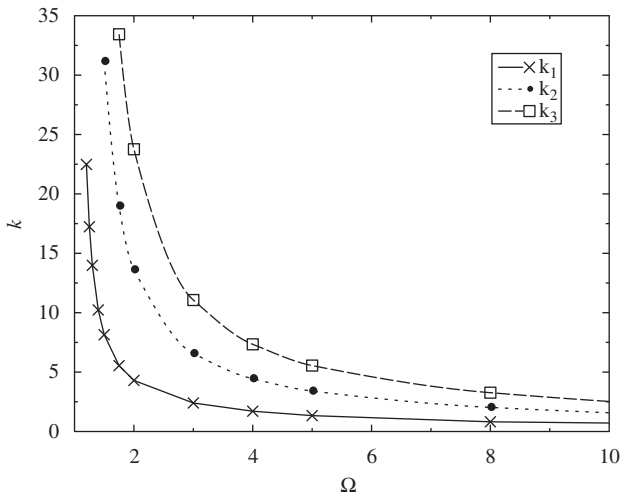

Fig. 3. As Fig. 2, for the odd mode $F_{1,2}$.

where u, v are, respectively, x-, y-components of the acoustic velocity perturbation, p is the acoustic pressure perturbation, ρ_0, p_0 the background mass density, pressure and adiabatic sound speed equation (3a)

$$c^2 = \left(\frac{\partial p_0}{\partial \rho_0}\right), \tag{3a}$$

$$\frac{\mathrm{d}}{\mathrm{d}t} \equiv \frac{\partial}{\partial t} + U(y)\frac{\partial}{\partial x}, \tag{3b}$$

and the material derivative equation (3b) corresponds to a background unidirectional shear flow $\mathbf{U} = U(y)\mathbf{e}_x$. A steady unidirectional shear mean flow leads to a constant pressure in the momentum equations (1a) and (1b), and satisfies the adiabatic continuity equation (2). The latter assumes isentropic conditions, so that the mass density $\rho(y)$ and sound speed $c(y)$ must be constant along streamlines (i.e. independent of x) but can vary transversely (i.e. be arbitrary functions of y consistent with the equation of state). In the case of an homentropic steady unidirectional shear flow the entropy is constant as well as the pressure, and thus the mass density and sound speed are also constant. Since an unidirectional shear flow leads to zero divergence for the velocity, there is no dilatation, and the preceding remarks hold irrespective of the Mach number. In the sequel is considered the acoustics of a steady homentropic unidirectional shear flow with unrestricted Mach number, for which elimination between Eqs. (1a), (1b) and (2) leads to [78] the following wave equation for the pressure:

$$\left\{\frac{1}{c^2}\frac{\mathrm{d}^2}{\mathrm{d}t^2} - \nabla^2\right\}\left(\frac{\mathrm{d}p}{\mathrm{d}t}\right) + 2U'\frac{\partial^2 p}{\partial x \partial y} = 0; \tag{4}$$

in the absence of shear flow $U' \equiv \mathrm{d}U/\mathrm{d}y = 0$, it would reduce to the convected wave equation, in curly brackets.

Since the background flow is steady, and uniform in the x-direction, it is convenient to use a Fourier decomposition in time t, and also in the longitudinal coordinate x along the walls

$$p,v(x,y,t) = \iint_{-\infty}^{+\infty} P,V(k,\omega;y)\mathrm{e}^{\mathrm{i}(kx-\omega t)}\,\mathrm{d}k\,\mathrm{d}\omega, \tag{5}$$

where P, V are, respectively, the acoustic pressure and normal velocity spectra, for a wave of frequency ω and longitudinal wavenumber k, at distance y from the axis. Substituting Eq. (5) in Eq. (4) leads to

$$(\omega - kU)P'' + 2kU'P' + (\omega - kU)\left[\frac{(\omega - kU)^2}{c^2} - k^2\right]P = 0, \tag{6}$$

where prime denotes derivative with regard to y, viz. $P' \equiv \mathrm{d}P/\mathrm{d}y$. The acoustic wave equation (6) can be written in the form

$$\omega_* P'' - 2\omega_*' p' + \omega_*\left(\frac{\omega_*^2}{c^2} - k^2\right)P = 0, \tag{7}$$

where ω_* denotes (Eq. (8a)) the Doppler shifted frequency:

$$\omega_*(y) = \omega - kU(y), \tag{8a}$$

$$\omega_*(y_c) = 0, \tag{8b}$$

emphasizing that where the latter vanishes (Eq. (8b)), there is a critical level $y = y_c$, which is a singularity of the wave equation.

To derive boundary conditions, Eqs. (5) are used in the y-component (Eq. (1b)) of the momentum equation

$$\frac{\mathrm{d}P}{\mathrm{d}y} = \mathrm{i}\rho[\omega - kU(y)]V = \mathrm{i}\rho\omega_* V. \tag{9}$$

An impedance condition is used to relate the acoustic pressure P and velocity V at the walls:

$$P(\pm L;k,\omega) = \pm Z^{\pm}(\omega)\, V(\pm L,k,\omega), \tag{10}$$

where the impedance may be different $Z^{\pm}$ at the two walls $y = \pm L$, and may depend on frequency ω and longitudinal wavenumber k. Thus the impedance boundary conditions reads

$$[\pm Z^{\pm} P' - \mathrm{i}\rho\omega P]_{y = \pm L} = 0. \tag{11}$$

In the case of elastic, i.e. compliant but non-absorbing wall, the impedance is imaginary

$$Z^{\pm} = \mathrm{i}|Z^{\pm}| : \quad [\pm |Z^{\pm}| P' - \rho\omega P]_{y = \pm L} = 0, \tag{12}$$

and the boundary condition equation (12) has real coefficients. A rigid wall corresponds to an infinite impedance

$$|Z^{\pm}| = \infty : \quad P'(\pm L;k,\omega) = 0, \tag{13}$$

and thus to zero normal gradient of the acoustic pressure at the wall.

3. Existence of critical level for parabolic shear flow

The boundary condition equations (9)–(13) are of Sturm–Liouville type

$$a_{\pm}P(\pm L;k,\omega)+b_{\pm}P'(\pm L;k,\omega)=0, \tag{14}$$

where $a_{\pm}$ and $b_{\pm}$ are constants; also as will be inferred in Section 8, the wave equation (7), when multiplied by ω_*^{-3}

$$\omega_*^{-2}P''-2\omega_*'\omega_*^{-3}P'+\left[\frac{1}{c^2}-\left(\frac{k}{\omega_*}\right)^2\right]P=0 \tag{15}$$

takes the self-adjoint form

$$\frac{\mathrm{d}}{\mathrm{d}y}\left\{G(y)\frac{\mathrm{d}P}{\mathrm{d}y}\right\}-[J(y)-\lambda H(y)]P=0, \tag{16}$$

where

$$G(y)=[\omega_*(y)]^{-2}=H(y), \tag{17a}$$

$$-J(y)=c^{-2}, \tag{17b}$$

$$-\lambda\equiv k^2. \tag{17c}$$

If critical levels are excluded $\omega_*(y)>0$ then $G(y)>0$ which is one condition of validity of Sturm's oscillation theorem [113]: for each positive integer, there is only one solution $P_n(y)$ of Eqs. (16) and (14) with n zeros in $-L\le y\le L$ and this eigenfunction corresponds to the eigenvalue λ_n. In the presence of a critical level $\omega_*(y_c)$, the function (17a) is singular at $y=\pm y_c$, but it is continuous and positive in sub-intervals (y_1, y_2) and (y_3, y_4) with $L>y_1>y_2>y_c>y_3>y_4>0$, and this meets one of the conditions of validity of the Klein oscillation theorem [113], where λ is replaced by $\lambda+\mu y$: for each pair of positive integers n, m, there is one pair of eigenfunctions, P_n with n zeros in (y_1, y_2) and Q_m with m zeros in (y_3, y_4), corresponding to unique eigenvalues, respectively, λ_n, μ_m. The eigenvalue would be $\lambda=-k^2$ in Eq. (17c), and the oscillation theorems require [113] that the functions in Eqs. (17a) and (17b) and coefficients equation (14) do not depend on λ; this is false here, since G, H in Eq. (17a) depend on $k=\sqrt{-\lambda}$ through the Doppler shifted frequency equation (8a). Thus the classical oscillation theorems of Sturm and Klein fail to apply to the present problem, and do not prove that eigenvalues and eigenfunctions exist in the present case; similarly, theorems on orthogonality and completeness of eigenfunctions may fail.

As a method to seek to determine eigenvalues and eigenfunctions, if they exist, the acoustic pressure is represented as a linear combination:

$$P(y;k,\omega)=C_1(k,\omega)E(y;k,\omega)+C_2(k,\omega)F(y;k,\omega), \tag{18}$$

of even E and odd F functions:

$$E(y)=E(-y), \tag{19a}$$

$$F(y)=-F(-y); \tag{19b}$$

symmetric boundary conditions are assumed. In the case of rigid walls, the boundary condition at $y=L$ is

$$0=P'(L)=C_1E'(L)+C_2F'(L), \tag{20a}$$

and at $y=-L$ is

$$0=P'(-L)=-C_1E'(L)+C_2F'(L), \tag{20b}$$

where the fact that E, F' are even and F, E' are odd has been used. In order that the solutions be non-trivial

$$\{C_1,C_2\}\neq\{0,0\}: \quad E'(L)F'(L)=0. \tag{21}$$

On the other hand, since E, F are linearly independent solutions of a linear second-order differential equation, their Wronskian is non-zero

$$0\neq\begin{bmatrix}E(y) & F(y)\\ E'(y) & F'(y)\end{bmatrix}=E(L)\ F'(L)-F(L)\ E'(L). \tag{22}$$

Thus $E'(L)=0=F'(L)$ cannot vanish at the same time, i.e.: (i) either $E'(L)=0\neq F'(L)$, and then $C_2=0$ by Eqs. (20a) and (20b) and the solution Eq. (18) is $P=C_1E(y)$ even; (ii) or $F'(L)=0$ and the solution is odd. Thus solutions can be sought which are either even or odd, and they can be used to find eigenvalues and eigenfunctions.

Consider next a parabolic shear flow, with velocity $U_0=U(0)$ on the axis of the duct, and zero at the walls $U(\pm L)=0$:

$$U(y)=U_0\left(1-\frac{y^2}{L^2}\right), \tag{23a}$$

$$U'(y) = -2U_0 \frac{y}{L^2} \equiv q(y), \tag{23b}$$

for which the vorticity increases linearly (in modulus) from zero on axis to $\pm 2U_0/L$ at the walls. The Doppler shifted frequency equations (8a) and (23a)

$$\omega_*(y) = \omega - U_0 k + U_0 k \frac{y^2}{L^2}, \tag{24}$$

vanish (8b) at the critical level(s)

$$y_c = \pm L\sqrt{1-\Lambda}, \tag{25a}$$

$$\Lambda \equiv \frac{\omega}{kU_0}, \tag{25b}$$

showing there are four cases: (i) for horizontal wavevector anti-parallel to the mean flow velocity $k<0$ with $\omega = kU_0$, the Doppler shifted frequency equation (24) is positive $\omega_* > 0$ in the flow region $L > |y| > 0$, except on axis $\omega_*(0) = 0$ where it vanishes, and a single critical level y_c occurs; (ii) for horizontal wavevector anti-parallel to the mean flow velocity $k<0$, since $\Lambda < 0$ the Doppler shifted frequency is positive in whole flow region $\omega_*(y) \geq \omega > 0$ and there are two critical levels at $y_c = \pm L\sqrt{1+|\Lambda|}$ outside the duct; (iii) for horizontal wavevector parallel to the mean flow velocity $k>0$ and Doppler shifted frequency positive on the axis $\omega > kU_0$, and hence everywhere $\omega_*(y) \geq \omega - kU_0$ since $\Lambda > 1$ and the critical levels lie at 'imaginary distance' $y_c = \pm \mathrm{i}\sqrt{\Lambda-1}$; (iv) for horizontal wavevector parallel to the mean flow velocity $k>0$ and negative Doppler shifted frequency on the axis of the duct $\omega_*(0) = \omega - kU_0 < 0$ since it is positive (and equal to the wave frequency) at the wall $\omega_*(\pm L) = \omega > 0$, it vanishes at two points in the duct for $\Lambda < 1$, which are the critical levels (25a). Each of four cases in addressed next in turn.

4. Case I: coincidence of singularities or critical levels on the axis of the duct

Substituting the parabolic velocity profile equation (23a) in the acoustic wave equation (6), or the Doppler shifted frequency equation (24) in the alternate form Eq. (7) of the wave equation, leads to a second-order linear differential equation, specifying the dependence of the acoustic pressure on distance from the axis:

$$[L^2(\Lambda-1)+y^2]P'' - 4yP' + \left(\Lambda - 1 + \frac{y^2}{L^2}\right)K^2 \left\{ \left(\Lambda - 1 + \frac{y^2}{L^2}\right)^2 M^2 - 1 \right\} P = 0; \tag{26}$$

it involves three dimensionless parameters, namely the wavenumber equation (27a), Mach number equation (27b):

$$K \equiv kL, \tag{27a}$$

$$M = U_0/c, \tag{27b}$$

and either Eq. (25b) or the dimensionless frequency:

$$\Omega \equiv \frac{\omega L}{c} = \Lambda KM. \tag{27c}$$

The dimensionless frequency Ω and wavenumber K can be given other interpretations. For the dimensionless frequency:

$$\Omega \equiv \frac{\omega L}{c} = \frac{2\pi L}{\tau c} = \frac{2\pi L}{\lambda}, \tag{28a}$$

where $\tau = 2\pi/\omega$ is the wave period, and $\lambda = \tau c$ the wavelength; thus Ω is a measure of the ratio of the half-width of the duct L to wavelength λ. Using

$$k = \frac{\omega}{c}\cos\theta, \tag{28b}$$

for the horizontal wavenumber, where θ would be the angle of the wavevector with the axis, if the medium were at rest, it follows that the dimensionless wavenumber is given by

$$K = kL = \frac{\omega L}{c}\cos\theta = \Omega\cos\theta; \tag{28c}$$

thus it specifies the angle of the direction of propagation with the mean flow. The parameter equation (27c)

$$\Lambda = \frac{\Omega}{KM} = \frac{1}{M\cos\theta} \tag{28d}$$

shows that one or two critical level(s) occur in the duct $\Lambda \geq 1$ iff the Doppler factor $1 - M\cos\theta \leq 0$ is non-positive.

Eq. (26) is simplest in the case $\Lambda = 1$ of critical level on the axis of the duct:

$$y^2 P'' - 4yP' + k^2 y^2 \left(\frac{M^2 y^4}{L^4} - 1\right) P = 0; \tag{29}$$

in this case there are only two independent parameters, e.g. K (Eq. (27a)) and Ω (Eq. (28a)), and then $M=\Omega/K$ by Eq. (27c). Performing the change of independent variable:

$$z=k^2y^2, \tag{30a}$$

$$P(y;k,\omega)=\Phi(z) \tag{30b}$$

reduces the order of the coefficients from six in the differential equation (29) to two in

$$z\Phi''-\frac{3}{2}\Phi'+\frac{1}{4}\left(\frac{\Omega^2}{K^6}z^2-1\right)\Phi=0, \tag{31}$$

where prime denotes derivative with regard to z. The point $z=0$ is a regular singularity of the differential equation (31), and thus a solution exists in the form of a Frobenius–Fuchs series:

$$\Phi(z)=z^\sigma\sum_{n=0}^{\infty}a_n(\sigma)z^n, \tag{32}$$

with index σ and coefficients a_n to be determined. The only other singularity of the differential equation (31) in the point at infinity $z=\infty$ which is an irregular singularity; hence the solution $\Phi(z)$ has an essential singularity as $z\to\infty$. This solution is not needed, since the radius of convergence of the series equation (32) is infinite, and therefore it covers the whole flow region. Substituting Eq. (32) into the differential equation (31), and equating to zero the coefficients of powers of z, follows the recurrence formula for the coefficients

$$4(n+\sigma)(n+\sigma-5/2)a_n=a_{n-1}-(\Omega/K^3)^2a_{n-3}; \tag{33}$$

the coefficients a_n with $n=-1,-2,\ldots$ negative integer are zero, because they are not present in Eq. (32). Setting $n=0$ in Eq. (33) yields the indicial equation:

$$\sigma(\sigma-5/2)a_0=0. \tag{34}$$

Now, if $a_0=0$ then $a_n=0$ by Eq. (33) for all $n=1,2,\ldots$, leading by Eq. (31) to a trivial solution $\Phi=0$. Thus one must set $a_0\neq0$; then the indicial equation (34) has roots $\sigma=0,5/2$. The root $\sigma=0$ corresponds an even solution:

$$E(y;k,\omega)=\Phi_0(z)=\sum_{n=0}^{\infty}a_n(0)\ (ky)^{2n}, \tag{35a}$$

and $\sigma=5/2$ to an odd solution:

$$F(y;k,\omega)=\Phi_{5/2}(z)=\sum_{n=0}^{\infty}a_n(5/2)\ (ky)^{2n+5}; \tag{35b}$$

the two solutions are linearly independent, and the general integral equation (18) is a linear combination, with arbitrary constants of integration C_1, C_2. The first coefficient $a_0(\sigma)$ in Eqs. (35) can be incorporated in C_1, C_2, i.e. one can set $a_0(0)=1=a_0(5/2)$, respectively, in Eqs. (35a) and (35b).

The even E and odd F solutions are plotted separately. The eigenvalues are the roots K_n of Eq. (13), viz. the eigenvalues of even equation (35a) and odd equation (35b) modes are given by the roots of, respectively,

$$0=LE'(\pm L)=\sum_{n=0}^{\infty}2na_n(0)(K)^{2n}, \tag{36a}$$

$$0=LF'(\pm L)=\sum_{n=0}^{\infty}(2n+5)a_n(5/2)(K)^{2n+5}; \tag{36b}$$

substituting the eigenvalues K_n in Eqs. (35a) and (35b), specifies the eigenfunctions E_n, $F_n(y)$. Note that each eigenvalue $K_n=k_nL$ in Eq. (27a) is a function of one free parameter, e.g. the dimensionless frequency Ω in Eq. (28a); since $\Lambda=1$, the Mach number is determined from the preceding. Real eigenvalues are considered for propagating waves and rigid walls (complex eigenvalues appear for impedance walls in Section 9). The first five eigenvalues K_1–K_5, of the even solution E, are given in Table 1 for several values of the dimensionless frequency Ω. Fig. 2 shows that the first two eigenvalues are close for $\Omega\geq2$, but the second eigenvalue K_2 increases rapidly for $\Omega<1.5$, whereas the first eigenvalue continues to decrease for $\Omega<1.5$; the next three eigenvalues K_3, K_4, and K_5 for the even eigenfunction follow a similar trend to K_2, increasing as Ω decreases. The first K_1, second K_2, and third K_3 eigenvalues for the odd solution F are given in Table 2, for several dimensionless frequencies; Fig. 3 shows that again the eigenvalues are closer for larger dimensionless frequency, and K_3 increases faster than K_1 as Ω reduces. The eigenfunctions of the even solution E are plotted, in Fig. 4 the eigenfunction E_1 corresponding to the first eigenvalue K_1, and in Fig. 5 the eigenfunction E_2 corresponding to the second eigenvalue K_2; for the odd mode, the eigenfunction F_1 corresponding to the first eigenvalue K_1 is plotted in Fig. 6, and the eigenfunction F_2 corresponding to the second eigenvalue K_2 is plotted in Fig. 7. All the eigenfunctions are plotted in Figs. 4–7 as a function of the dimensionless distance $Y\equiv y/L$, defined as the distance from the axis y divided by the half-width of duct L. It is clear that for high-frequencies $\Omega^2\gg1$ or (Eqs. (27c),

Table 1
First five eigenvalues $K_1(\Omega)-K_5(\Omega)$, as a function of dimensionless frequency $\Omega=\omega L/c$, for even mode $E(y)$ in the case I of horizontal wavevector parallel to the mean flow velocity with critical level on duct axis $\Lambda=1$.

Ω	K_1	K_2	K_3	K_4	K_5
0.25	1.282283	–	–	–	–
0.3	1.315564	–	–	–	–
0.4	1.393492	–	–	–	–
0.5	1.482212	–	–	–	–
0.6	1.577448	–	–	–	–
0.7	1.676097	–	–	–	–
0.75	1.726019	–	–	–	–
0.8	1.776080	–	–	–	–
1.0	1.975371	–	–	–	–
1.15	2.122194	32.173047	–	–	–
1.25	2.218604	17.232133	–	–	–
1.4	2.361482	10.230828	–	–	–
1.5	2.456172	8.1437346	31.15257	–	–
1.75	2.696838	5.5368196	18.97793	33.44000	–
2.0	2.973492	4.2418849	13.61542	23.75999	34.05562
2.1	3.134116	3.8302910	12.24353	21.28399	30.47445
2.2	–	–	11.13084	19.27647	27.57048
2.3	–	–	10.21116	17.61812	25.17130
2.4	–	–	9.438748	16.22650	23.15777
2.5	–	–	8.781027	15.04292	21.44511
3.0	–	–	6.556554	11.06610	15.69079
4.0	–	–	2.025681	7.334041	10.30830

Table 2
As Table 1, but concerning the first $K_1(\Omega)$, second $K_2(\Omega)$, and third $K_3(\Omega)$ eigenvalues, for the odd mode $F(y)$.

Ω	K_1	K_2	K_2
1.2	22.48272	–	–
1.25	17.23213	–	–
1.3	13.98583	–	–
1.4	10.23083	–	–
1.5	8.143831	31.15257	–
1.75	5.542838	18.97793	33.44000
2.0	4.297875	13.61542	23.75999
3.0	2.399447	6.561798	11.06614
4.0	1.708063	4.444399	7.338548
5.0	1.335727	3.400145	5.549440
8.0	0.815271	2.028624	3.266707
16.0	0.403147	0.992651	1.587943

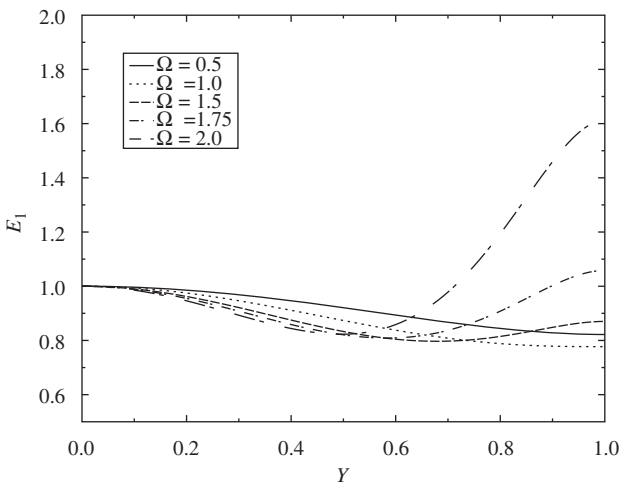

Fig. 4. Even eigenfunctions E_1, corresponding to first eigenvalue, plotted versus dimensionless distance from the axis $Y=y/L$, for case I horizontal wavevector parallel to the mean flow velocity with critical level on the duct axis.

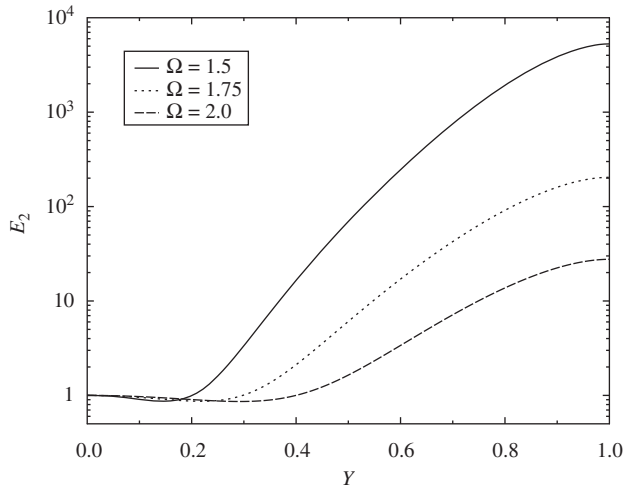

Fig. 5. As for Fig. 4, for even eigenfunctions E_2, corresponding to second eigenvalue K_2.

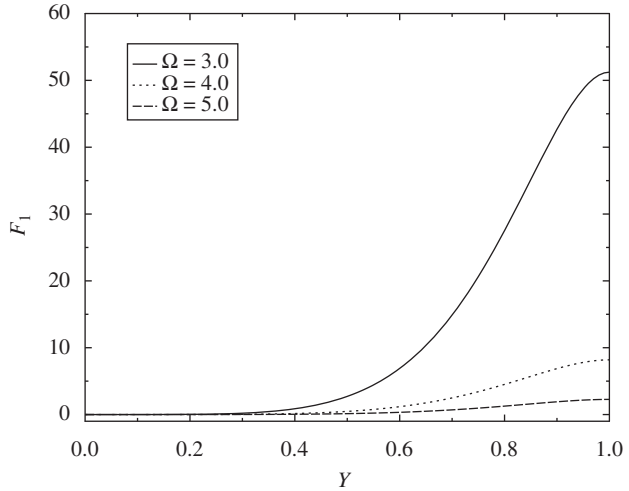

Fig. 6. As for Fig. 4, for first odd eigenfunction F_1.

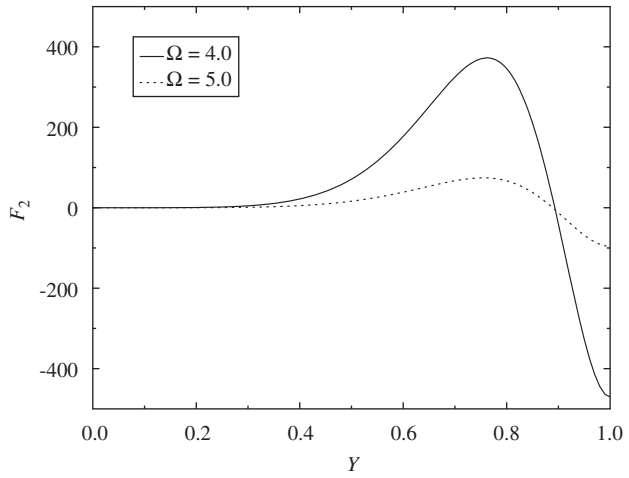

Fig. 7. As for Fig. 5, for second odd eigenfunction F_2.

(28a)) smaller wavelength compared with the width of the duct, the acoustic pressure is higher near the wall; this corresponds to the known result in ray theory, that sound is refracted away from regions of high velocity. For propagation downstream, the group velocity $c + U(y)$ is higher near the axis, and sound waves are refracted towards the wall [78]. At frequencies $\Omega \sim 1$ for which ray theory no longer holds, this need not be true, and cases of acoustic pressure smaller at the wall than on the axis of the duct occur in Figs. 4 and 7, i.e. both for even and some odd modes. In order to explain this, note that for even modes, the acoustic pressure $E'(0) = 0$ has an extremum at the centre of the duct; from Eq. (31) it follows that the sign of the second derivative E'' is determined by the factor in curved brackets. For high-frequencies this factor is positive, i.e. $E'' > 0$, so the acoustic pressure is minimum at the centre of the duct, and increases towards the walls; for low-frequencies $E'' < 0$ the acoustic pressure is maximum at the centre of the duct and decreases towards the walls, as seen in Fig. 4. Concerning the odd modes, the centre of the duct is an inflexion point $F(0) = 0 = F''$, and from Eq. (31) it follows that the slope is also zero there $F' = 0$; for small y the slope F' has the sign opposite to the factor in curved brackets, i.e. is positive and smaller for higher frequencies; thus higher frequencies correspond to smaller changes of acoustic pressure, as seen in Figs. 6 and 7.

5. Case II: critical levels outside the duct

In the general case $\Lambda \neq 1$, the wave equation (26) does not simplify to Eq. (29), and thus, instead of Eqs. (30a) and (30b) the following change of variable is performed:

$$\zeta = \frac{y^2}{L^2(1-\Lambda)}, \tag{37a}$$

$$P(y;k,\omega) = \Psi(\zeta) \tag{37b}$$

leading to a second-order linear differential equation whose coefficients are polynomials of degree up to three (instead of six):

$$(1-\zeta)\zeta\Psi'' + \left(\frac{1}{2} + \frac{3\zeta}{2}\right)\Psi' + (1-\zeta)\alpha[(1-\zeta)^2\beta - 1]\Psi = 0; \tag{38}$$

the independent dimensionless parameters are still the wavenumber equation (27a), Mach number equation (27b) and frequency equation (28a) or (25b), but they appear in Eq. (38) only in two combinations:

$$\alpha \equiv \frac{K^2(1-\Lambda)}{4} = \frac{K(K-\Omega/M)}{4}, \tag{39a}$$

$$\beta \equiv (1-\Lambda)^2 M^2 = \left(\frac{\Omega}{K} - M\right)^2. \tag{39b}$$

The change of variable in Eq. (37a) is such that the critical level(s) are by Eq. (25a) at the point unity equation (40a):

$$\zeta(\pm y_c) = 1 \tag{40a}$$

$$\zeta(\pm L) = \frac{1}{1-\Lambda}, \tag{40b}$$

and the position of the walls equation (40b) depends on $\Lambda = \omega/kU_0 = u/U_0$, which is the ratio of the phase speed of sound $u = \omega/k$ to the peak flow velocity U_0 (another interpretation is given by Eq. (28d). The wave equation (38) has regular singularities on the axis of the duct $\zeta = 0$, and at the critical level(s) $\zeta = 1$, and an irregular singularity at infinity $\zeta = \infty$; it is of the extended of Gaussian hypergeometric type:

$$(1-\zeta)\zeta\Psi'' + \{\gamma - (\alpha+\beta+1)\zeta\}\Psi' - \left(\alpha\beta + \sum_{m=1}^{s} A_m \zeta^m\right)\Psi = 0, \tag{41}$$

where (i) for the Gaussian hypergeometric type $s = 0$, the point at infinity is a regular singularity; (ii) in the case of sound in an exponential shear flow [89] $s = 2$, the point at infinity $\zeta = \infty$ is an irregular singularity of degree two, and the solution has an essential singularity, which can be specified by normal integrals [116,117]; (iii) in the present case, of sound in a parabolic shear flow equation (38), the point at infinity is an irregular singularity of third degree $s = 3$ and the same procedure shows that method of normal integrals generally fails and a Laurent series solution is needed (Appendix A).

In the case II of horizontal wavevector anti-parallel to the mean flow velocity $K < 0$ since $\Lambda < 0$, and the critical levels $\zeta(y_c) = 1 > \zeta(\pm L) = 1/(1-\Lambda)$ lie outside the duct, implying that the Frobenius–Fuchs expansion around the axis of the duct $\zeta = 0$, which is valid for $|\zeta| < 1$, covers the whose flow region $|\zeta| \leq \zeta(\pm L) < 1$. The details are similar to case I in Section 4, i.e. the substitution:

$$\Psi_\sigma(\zeta) = \zeta^\sigma \sum_{n=0}^{\infty} b_n(\sigma)\, \zeta^n, \tag{42}$$

in Eq. (38) leads to the recurrence formula for the coefficients:

$$(n+\sigma)(n+\sigma-1/2)b_n = [(n+\sigma-1)(n+\sigma-7/2) + \alpha(\beta-1)]b_{n-1} - \alpha(1-3\beta)b_{n-2} - 3\alpha\beta b_{n-3} + \alpha\beta b_{n-4}, \tag{43}$$

and for $n=0$, the indicial equation:

$$\sigma(\sigma-1/2)b_0=0. \tag{44}$$

The root $\sigma=0$ corresponds to an even, and $\sigma=1/2$ to an odd, solution:

$$E(y)=\Psi_0(\zeta)=\sum_{n=0}^{\infty} b_n(0)(1-\Lambda)^{-n}\left(\frac{y}{L}\right)^{2n}, \tag{45a}$$

$$F(y)=\Psi_{1/2}(\zeta)=\sum_{n=0}^{\infty} b_n(1/2)(1-\Lambda)^{-n-1/2}\left(\frac{y}{L}\right)^{2n+1}. \tag{45b}$$

The eigenvalues for the even equation (45a) and odd equation (45b) solutions are given, respectively, by the roots K_n of

$$0=LE'(\pm L)=\sum_{n=0}^{\infty} b_n(0)(1-\Lambda)^{-n}2n, \tag{46a}$$

$$0=LF'(\pm L)=\sum_{n=0}^{\infty} b_n(1/2)(1-\Lambda)^{-n-1/2}(2n+1); \tag{46b}$$

substituting K by K_n in Eqs. (45a) and (45b) leads to the eigenfunctions for the even E_n and odd F_n modes. These solutions cover the whole flow region, because for $kU(y)<0$, the Doppler shifted frequency equation (8a) is greater than wave frequency $\omega_*(y)>\omega$ and thus it cannot vanish in the flow region, i.e. there are no critical levels inside the duct; the critical levels $\zeta=1$ or Eq. (25a) at $y_c=\pm L\sqrt{1+|\Lambda|}$ outside the duct, correspond to a velocity profile Eq. (23a) extended into a region $|y|>L$ of 'back flow' $U(y)<0$ so that then the horizontal wavevector is parallel to the mean flow velocity, and the Doppler shifted frequency vanishes, although this occurs outside the region of interest.

The eigenvalues K_n depend on the remaining two free parameters, e.g. the dimensionless frequency equation (28a) and the Mach number equation (27a). The first eigenvalue K_1 of the even mode E_1 is given in Tables 3 and 4, for several values of the dimensionless frequency and, respectively, subsonic and supersonic Mach numbers; in the present case II, of propagation upstream, the group velocity $c-U(y)$ is smaller near the axis, and ray theory predicts that at high-frequencies $\Omega^2\gg 1$, the sound is refracted away from the region of high group velocity, near the walls; at low frequencies, the acoustic pressure is higher near the walls, as had been found in the preceding case (Section 4). Figs. 8 and 9 show plots of the first even eigenfunction E_1 for several values, respectively, of the subsonic Mach number and dimensionless frequency. It is clear from Fig. 9 that for the even mode and case II, the acoustic pressure is lower at the walls than at the centre of the duct, with this effect being more pronounced at higher frequencies; Fig. 8 shows that an increase in the Mach number of the background flow, which causes a larger variation of group velocity $c(1-M)$ across the duct, has a similar effect to an increase in frequency,

Table 3
First eigenvalue $K_1(\Omega,M)$, as a function of Mach number M and dimensionless frequency Ω for the even mode $E_1(y)$ in case II of horizontal wavevector anti-parallel to the mean flow velocity with no critical levels in the flow.

Ω	$M=0.1$	$M=0.3$	$M=0.5$	$M=0.7$	$M=0.8$
0.1	−0.10698	−0.12302	−0.14209	−0.16441	−0.17681
0.5	−0.53495	−0.61558	−0.71292	−0.83129	−0.90081
0.6	−0.64196	−0.73895	−0.85688	−1.00292	−1.09116
0.8	−0.85600	−0.98615	−1.14727	−1.35673	−1.49393
1.0	−1.07009	−1.23410	−1.44195	−1.73084	−1.94488
2.0	−2.14156	−2.49209	−3.02853	−4.30951	−6.26723
4.0	−2.76462	−3.43260	−4.16657	−5.03731	−5.73790
8.0	−5.52611	−6.89825	−8.38210	–	–

Table 4
As Table 3, for supersonic flow.

Ω	$M=1.2$	$M=1.8$	$M=2.0$	$M=2.5$
0.1	−0.23441	−0.34360	−0.38742	−0.54049
0.5	−1.35184	−5.05152	−4.21520	−2.97937
0.6	–	−4.90989	−4.08762	−2.84264
0.8	–	−4.61348	−3.80806	−2.43460
1.0	–	−4.28754	−3.46328	−1.61414
2.0	−8.83741	−1.00831	−0.87457	−0.66633
4.0	–	−2.16786	−1.87798	−1.42847
8.0	−2.03341	−1.24264	−1.10568	−0.86980

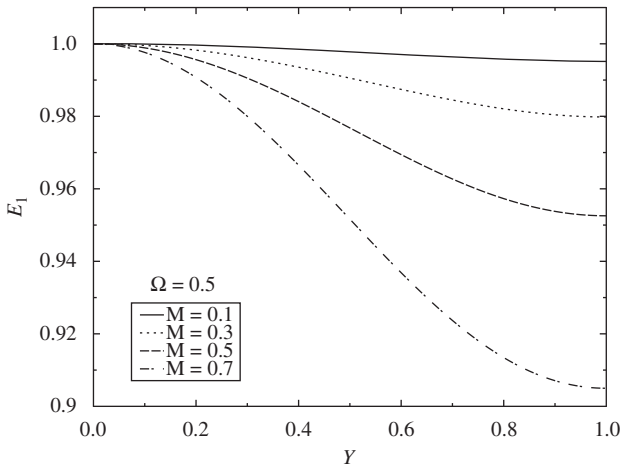

Fig. 8. First even eigenfunction E_1, as a function of dimensionless distance from axis $Y = y/L$, for fixed dimensionless frequency $\Omega = 0.5$, and several values of Mach number M, for case II of horizontal wavevector anti-parallel to the mean flow velocity.

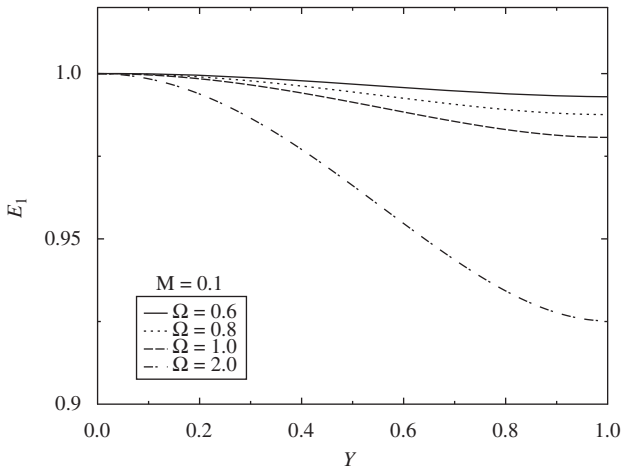

Fig. 9. As Fig. 8, for fixed Mach number $M = 0.1$, and several values of dimensionless frequency Ω.

Table 5
As Table 3, for the odd mode $F_1(y)$.

Ω	$M = 0.1$	$M = 0.3$	$M = 0.5$	$M = 0.7$	$M = 0.8$
2.0	−1.38668	−1.71427	−2.07839	−2.50166	−2.76286
4.0	−3.89925	−4.42990	−5.25030	−7.36135	−2.24163
8.0	−2.15966	−3.96192	−6.27548	−8.52873	−9.66646

i.e. a larger excess of acoustic pressure at the axis of the duct, when compared with the wall values, occurs for higher Mach numbers. Concerning the odd mode, the first eigenvalue is indicated for several frequencies in Table 5 for subsonic and Table 6 for supersonic flows. For the first odd eigenfunction, the acoustic pressure at the wall increases with increasing subsonic Mach number (Fig. 10) and decreasing frequency (Fig. 11), the effect being weaker than for the even mode. The first even and odd eigenfunctions are plotted, respectively, in Figs. 12 and 13 for several dimensionless frequencies and one of the supersonic Mach numbers in Tables 4 and 6. Fig. 12 shows a pressure oscillation of the first even mode between the duct axis and the wall at lower frequencies; there is a monotonic decay towards the wall, as predicted by ray theory, only for the higher dimensionless frequency. The pressure oscillations also appear for the first odd mode F_1 in Fig. 13, more noticeably at higher dimensionless frequencies; for small dimensionless frequency there is a monotonic pressure increase towards the wall, from the zero at the duct axis.

Table 6
As Table 5, for supersonic flow.

Ω	$M=1.2$	$M=1.5$	$M=1.8$	$M=2.0$
0.1	–	−5.25382	−3.65934	−3.08515
0.3	–	−4.86016	−3.37211	−2.81835
0.5	−9.34363	−4.45312	−3.04091	−2.46752
0.6	−8.86316	−4.24007	−2.83755	−2.17589
0.8	−7.90844	−3.77293	−0.64931	−0.53688
1.0	−6.95966	−0.54519	−0.41466	−0.36166
2.0	–	−7.19973	−4.54283	−2.84041
4.0	−0.97970	−0.74138	−0.60160	−0.53559
8.0	−5.27047	−3.53456	−2.76263	−2.42704

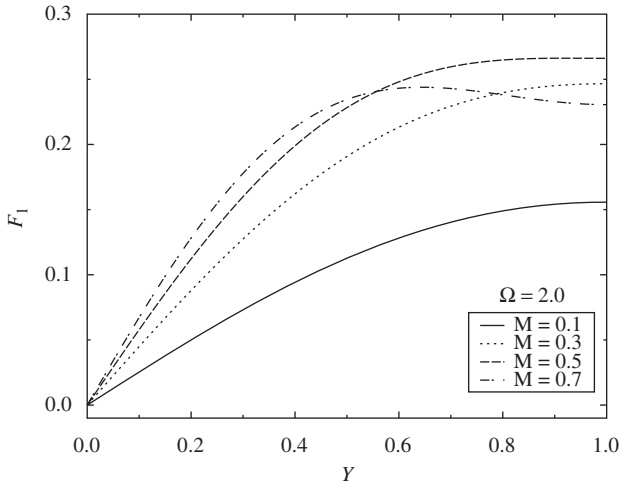

Fig. 10. As Fig. 8, for first odd eigenfunction F_1.

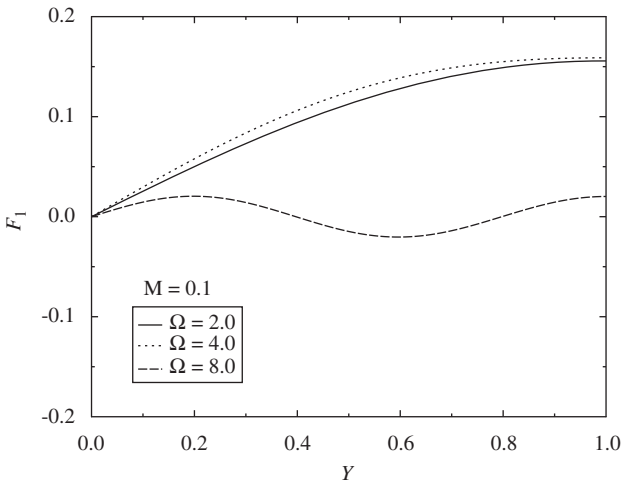

Fig. 11. As Fig. 9, for the first odd eigenfunction F_1.

6. Case III: imaginary critical levels and matching of solutions

In the case of horizontal wavevector anti-parallel to the mean flow velocity there is never a critical level in the flow region, i.e. they lie outside the walls, and do not limit the convergence of the solution about the axis of the duct, in the region of interest, namely, the duct. In the case of horizontal wavevector parallel to the flow velocity $k>0$, there is no critical level if the Doppler shifted frequency is positive throughout the flow region $\Lambda>1$ in Eq. (25b), i.e. the critical level equation (25a) lies at

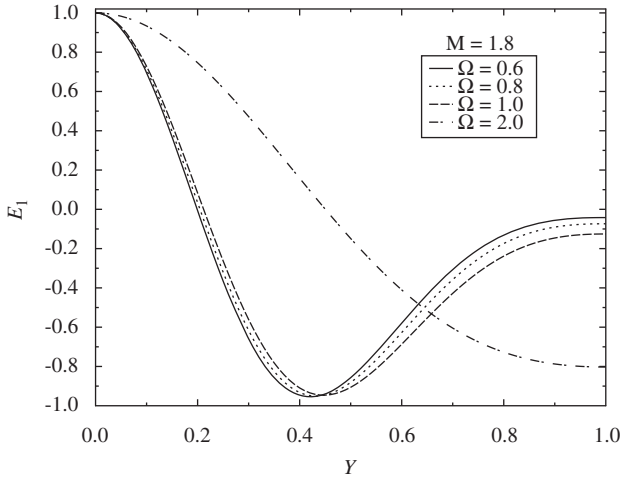

Fig. 12. First even eigenfunction E_1, as a function of dimensionless distance from axis $Y = y/L$, for fixed Mach number $M = 1.8$, and several values of dimensionless frequency, for case II of horizontal wavevector anti-parallel to the mean flow velocity.

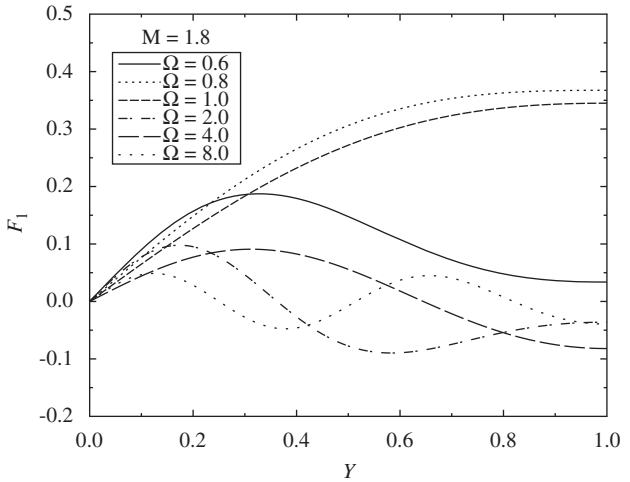

Fig. 13. First even eigenfunction F_1, as a function of dimensionless distance from axis $Y = y/L$, for fixed Mach number $M = 1.8$, and several values of dimensionless frequency, for case II of horizontal wavevector anti-parallel to the mean flow velocity.

imaginary 'distance' equation (47a):

$$y_c = \pm \mathrm{i} L\sqrt{\Lambda - 1}, \tag{47a}$$

$$0 \leq |y_c| = L\sqrt{\Lambda - 1}, \tag{47b}$$

although then the solution equations (45a), (45b) and (43) are limited in their radius of convergence (47b) by this location. If $\Lambda \geq 2$, i.e. $\omega \geq 2kU_0$ and $|y_c| \geq L$, the solution equations (45a) and (45b) cover the whole flow region; if $1 \leq \Lambda < 2$ they cover only a part of the flow region equation (47b) near the axis of the duct, and they must be matched to another pair of solutions, covering a region near the wall, overlapping with Eq. (47b), i.e. valid for $y_1 \leq |y| \leq L$, with $y_1 < |y_c|$. The solution about the irregular singularity at infinity $y = \pm\infty$, $z = \infty$, is complicated since it has an essential singularity of non-normal type (Appendix A), and besides holds only for $|y| > |y_c|$ i.e. it does not overlap with Eq. (47b), except possibly at $|y| = |y_c|$ if the equality sign holds in both cases. It is more practical to seek a pair of solutions around a regular point y_0, since the y_c is on the imaginary axis, it is farther from real y_0 than the origin, which is the other singularity at finite distance. Thus choosing:

$$y_0 = \frac{L}{\sqrt{2}}, \tag{48a}$$

$$\zeta_0 = \frac{1}{2(1-\Lambda)} < 0, \tag{48b}$$

the solution about the regular point $y=y_0$ has radius of convergence $y_0=L/\sqrt{2}$ and thus applies over a region $0<y<2y_0=L\sqrt{2}$ which includes the wall. This suggests the introduction of the new variable equation (49a):

$$\eta=\zeta-\zeta_0, \tag{49a}$$

$$|\zeta-\zeta_0|<-\zeta_0,1-\zeta_0, \tag{49b}$$

leading to a power series solutions converging for Eq. (49b). It can be confirmed that these conditions are met by Eq. (48b), viz:

$$\frac{1}{1-\Lambda}<2\zeta_0,\quad 2\zeta_0-1<\zeta<0<-2\zeta_0,\quad 1-2\zeta_0<\frac{1}{\Lambda-1}, \tag{50}$$

because for $\Lambda>1$, it follows from Eq. (37a), over the whole duct except the axis $0<|y|\leq L$, that $0>\zeta>1/(1-\Lambda)$, in agreement with Eq. (50).

The change of variable:

$$\eta=\zeta+\frac{1}{2(\Lambda-1)}, \tag{51a}$$

$$\Psi(\zeta)=Q(\eta), \tag{51b}$$

transforms the wave equation (38) to

$$(1-\zeta_0-\eta)(\zeta_0+\eta)Q''+\left\{\frac{1+3\zeta_0+3\eta}{2}\right\}Q'+\{\alpha(1-\zeta_0-\eta)[\beta(1-\zeta_0-\eta)^2-1]\}Q=0. \tag{52}$$

The power series solution is sought in the Frobenius–Fuchs form

$$Q_\sigma(\eta)=\eta^\sigma\sum_{n=0}^{\infty}d_n(\sigma)\eta^n, \tag{53}$$

viz, although a MacLaurin series solution $\sigma=0$ exists, retaining the index $\sigma\neq0$ facilitates calculating the coefficients; the latter satisfy the recurrence relation:

$$\begin{aligned}(n+\sigma)(n+\sigma-1)\zeta_0(1-\zeta_0)d_n+(n+\sigma-1)[(n+\sigma-2)(1-2\zeta_0)+(1+3\zeta_0)/2]d_{n-1}\\ =\{(n+\sigma-2)(n+\sigma-9/2)+\alpha(1-\zeta_0)[1-\beta(1-\zeta_0)^2]\}d_{n-2}\\ +\alpha[1-3\beta(1-\zeta_0)^2]d_{n-3}+3\beta\alpha(1-\zeta_0)d_{n-4}+\beta\alpha d_{n-5}\end{aligned} \tag{54}$$

for $n=0$ the indicial equation is obtained

$$(\sigma-1)\sigma\zeta_0(1-\zeta_0)d_0=0, \tag{55}$$

whose roots are $\sigma=0,1$. The higher root leads to the solution:

$$Q_1(\eta)=\sum_{n=0}^{\infty}d_n(1)\left\{\left[\left(\frac{Y}{L}\right)^2-\frac{1}{2}\right]\frac{1}{(1-\Lambda)}\right\}=T(y), \tag{56}$$

for which the recurrence formula equation (54) specifies all coefficients. Note that the solution equation (56) is even in y, and the solution of Eq. (53) with $\sigma=0$ would also be even; thus the latter solution $Q_0(\eta)$ must reduce to a constant multiple of $Q_1(\eta)$, and this can be shown to be the case in the usual way [116], noting that the coefficient of d_1 vanishes in Eq. (54) for $\sigma=0$, $n=0$ in Eq. (54), i.e. d_2 cannot be determined from d_0. The procedure is similar to that used in Appendix B, and as in that case the second linearly independent solution $S(y)$ has a logarithmic singularity $\log(\zeta-\zeta_0)$ at $\zeta=\zeta_0$ which introduces a phase term. A similar situation will occur in the next section (Section 7), where the method to deal with such logarithmic singularities will be presented in more detail.

Since the pairs of solutions E, F (Eqs. (45a) and (45b)) of Eq. (38) and T, S of Eq. (52) are valid over an overlapping region $|\zeta|<1$ and Eq. (50):

$$|\zeta|<\min\{1,1/(\Lambda-1)\}, \tag{57a}$$

$$|y|<\min\{L,L\sqrt{\Lambda-1}\}, \tag{57b}$$

they are related by a linear combination:

$$E(y)=A_{11}T(y)+A_{12}S(y), \tag{58a}$$

$$F(y)=A_{21}T(y)+A_{22}S(y), \tag{58b}$$

with constant coefficients $A_{11},A_{12},A_{21},A_{22}$ which can be determined at any two points. The case III corresponds to horizontal wavevector parallel to the mean flow velocity and critical layer at a distance $\Lambda\geq2$ such that the solution equations (45a) and (45b) cover the whole flow region. The eigenvalues are determined by Eqs. (46a) and (46b) for $\Lambda\geq2$ and by substitution of Eqs. (58a) and (58b) in $E(L)=0=F(L)$ for $1<\Lambda<2$. The first eigenvalues in cases II–IV depend on Mach number equation (27b) and dimensionless frequency equation (28a). The first eigenvalue K_1 for the even mode $E_1(y)$ is given in Table 7 for fixed frequency Ω and several Mach numbers M, and for the odd mode $F_1(y)$ in Table 8; it follows that the eigenvalue K_1 of E_1

Table 7
First eigenvalue $K_1(\Omega,M)$, as a function of Mach number $M=U_0/c$ on the axis of the duct and dimensionless frequency Ω, for the even mode $E_1(y)$, in the case III of horizontal wavevector parallel to the mean flow velocity.

Ω	$M=0.1$	$M=0.3$	$M=0.5$	$M=0.7$
0.1	0.09363	0.08257	0.07339	0.06576
0.5	0.46819	0.41293	0.36710	0.32894
0.6	0.56184	0.49555	0.44059	0.39480
0.8	0.74915	0.66088	0.58768	0.52666
1.0	0.93648	0.82633	0.73496	0.65876
2.0	1.87372	1.65655	1.47623	1.32494
4.0	2.22164	1.80727	1.49523	1.25902
8.0	4.45225	3.64261	3.03111	2.56477

Table 8
As Table 7, for the odd mode $F_1(y)$.

Ω	$M=0.1$	$M=0.3$	$M=0.5$	$M=0.7$	$M=0.8$
2.0	1.10167	0.87143	0.69747	0.57006	0.51983
4.0	3.47624	3.11080	2.78589	2.49582	2.36326
8.0	1.07644	0.60617	0.40239	0.29732	0.26245

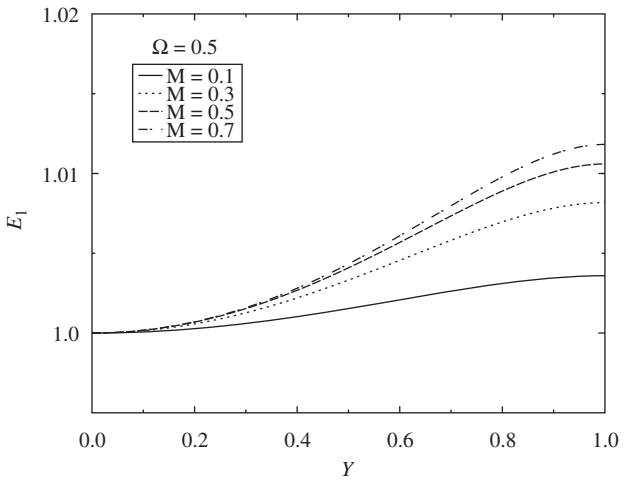

Fig. 14. First even eigenfunction E_1, as a function of dimensionless distance from axis $Y=y/L$ for fixed dimensionless frequency Ω, and several values of Mach number M, for case III of horizontal wavevector parallel to the mean flow velocity without critical levels in the flow region.

increases with increasing frequency Ω, and decreasing Mach number M. The first eigenfunction of the even mode E_1 is plotted in Fig. 14 for fixed frequency and several Mach numbers, and vice versa in Fig. 15: in all cases the acoustic pressure increases towards the wall, more so at higher Mach numbers and higher frequencies. The first eigenvalue for the odd and even modes is indicated in Table 9 for one dimensionless frequency and several Mach numbers including supersonic cases. The first even and odd eigenfunctions are plotted, respectively, in Figs. 16 and 17 for a high dimensionless frequency $\Omega=8.0$ and eight Mach numbers ranging from low sub-sonic to bissonic. The wave forms are oscillatory and not too sensitive to Mach number at this high frequency well into the ray limit $\Omega^2\gg 1$.

7. Case IV: two critical levels in the flow region

The remaining case IV corresponds to the horizontal wavevector parallel to the mean flow velocity $0<\Lambda<1$ when the Doppler shifted frequency changes sign between the axis of the duct $\omega_*(0)=\omega-kU_0<0$ and the walls $\omega_*(\pm L)=\omega>0$, and thus vanishes at two critical levels $\omega_*(y_c)=0$ in the stream equation (25a). The critical level can occur only for horizontal wavevector parallel to the mean flow velocity, which reduces the Doppler the shifted frequency relative to the wave frequency $\omega_*(0)<\omega$ and where the phase speed $\omega/k=U(y_c)$ equals the mean flow velocity. Since the two critical levels $y=\pm y_c$ in Eq. (26), coalesce to a single point unity $\zeta_c=1$ in terms of the variable in Eq. (37a), they can be placed at the origin,

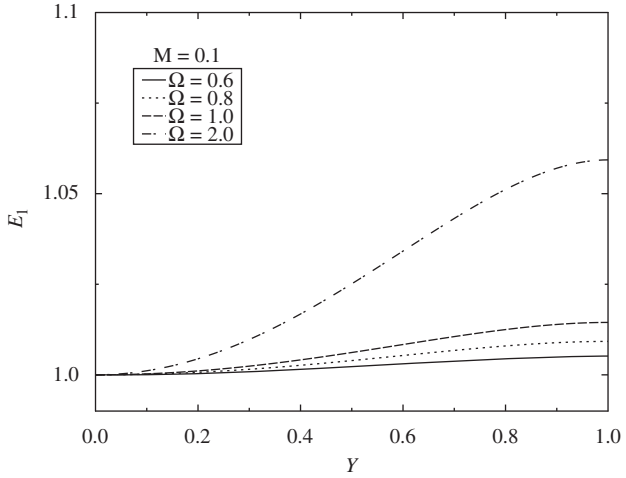

Fig. 15. As Fig. 14, for a fixed Mach number M, and several values of dimensionless frequency Ω.

Table 9
First eigenvalue $K_1(\Omega,M)$, as a function of Mach number $M = U_0/c$ on the axis of the duct for dimensionless frequency $\Omega = 0.8$, for the even $E_1(y)$ and odd $F_1(y)$ modes, in the case III of horizontal wavevector parallel to the mean flow velocity.

M	Even mode	Odd mode
0.8	2.37337	0.262459
1.2	1.80349	0.177899
1.8	1.30133	0.119509
2.0	1.18758	0.107685

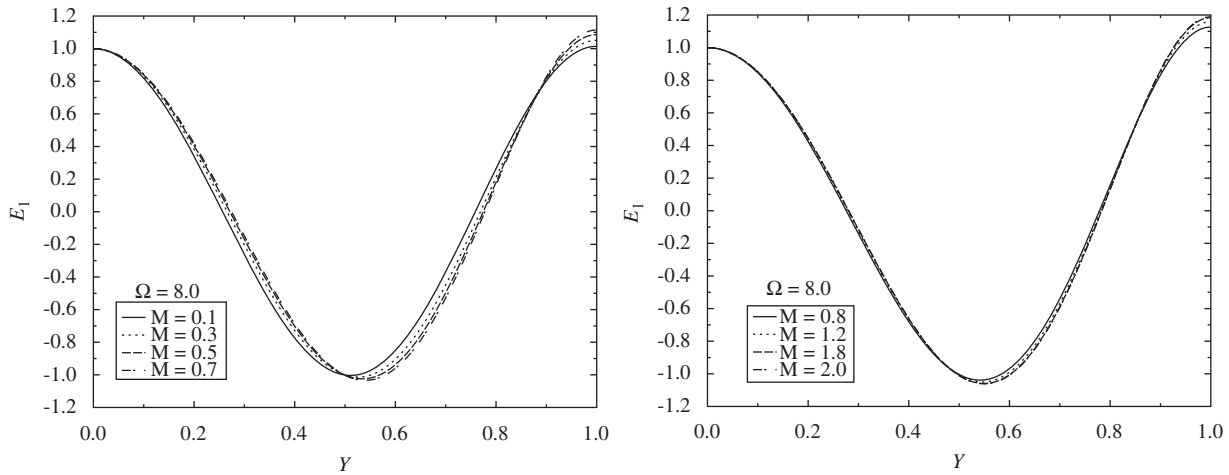

Fig. 16. First even eigenfunction E_1, as a function of dimensionless distance from axis $Y = y/L$ for fixed dimensionless frequency $\Omega = 8.0$, and several values of Mach number M, for case III of horizontal wavevector parallel to the mean flow velocity without critical levels in the flow region.

using the new variable

$$\xi \equiv 1-\zeta = 1-\frac{y^2}{L^2(1-\Lambda)}, \tag{59a}$$

$$\Psi(\zeta) = R(\xi), \tag{59b}$$

which transforms the wave equation (38) to

$$(1-\xi)\xi R'' + (\tfrac{3}{2}\xi - 2)R' + \alpha\xi(\xi^2\beta - 1)R = 0. \tag{60}$$

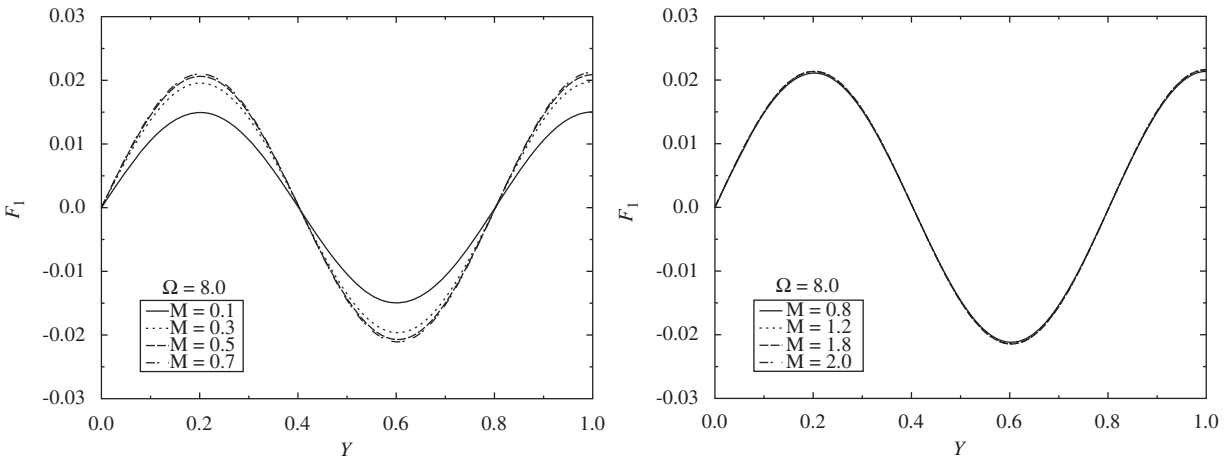

Fig. 17. Same as previous figures, but for first odd eigenfunction F_1.

Since the critical level $\xi = 0$ is a regular singularity, there is a power series solution

$$R_\sigma(\xi) = \xi^\sigma \sum_{n=0}^{\infty} e_n(\sigma)\ \xi^n, \tag{61}$$

which has unit radius of convergence $|\xi| < 1$, because the nearest singularity is the axis of the duct $\zeta = 0$, $\xi = 1$. Substitution of Eq. (61) into Eq. (60) leads to the recurrence formula for the coefficients

$$(n+\sigma)(n+\sigma-3)e_n(\sigma) = (n+\sigma-1)(n+\sigma-7/2)e_{n-1}(\sigma)+\alpha e_{n-2}(\sigma)-\alpha\beta e_{n-4}(\sigma), \tag{62}$$

and setting $n = 0$ specifies the indicial equation

$$\sigma(\sigma-3)e_0(\sigma) = 0. \tag{63}$$

The largest root $\sigma = 3$ leads to a solution

$$R_3(\xi) = \sum_{n=0}^{\infty} e_n(3)\ \xi^{n+3} = \sum_{n=0}^{\infty} e_n(3)\ \left[1-\frac{y^2}{L^2(1-\Lambda)}\right]^{n+3} \equiv W(y); \tag{64}$$

the index $\sigma = 0$ leads to a solution with a logarithmic singularity:

$$R_0(\xi) = R_3(\xi)\log\xi + \sum_{n=0}^{\infty} e_n(0)\xi^{n+3}, \tag{65}$$

of which details are given in Appendix B.

The logarithmic singularity has a jump across critical level:

$$\log\xi = \log\{1-(y/y_c)^2\} = \begin{cases} \log|1-(y/y_c)^2| & \text{if } |y| < y_c, \\ \log|1-(y/y_c)^2|-\mathrm{i}\pi & \text{if } |y| > y_c, \end{cases} \tag{66}$$

where it is necessary to justify why the phase term is $-\mathrm{i}\pi$ and not $+\mathrm{i}\pi$. To do so the standard procedure is followed [119,96], of giving the frequency a small positive imaginary part equation (67a):

$$\omega = \overline{\omega} + \mathrm{i}\varepsilon, \tag{67a}$$

$$\mathrm{e}^{-\mathrm{i}\omega t} = \mathrm{e}^{-\mathrm{i}\overline{\omega} t}\mathrm{e}^{\varepsilon t}, \tag{67b}$$

causing a growth in time in Eq. (5), viz. Eq. (67b) for $\varepsilon > 0$ as would be the case in the slow triggering of an instability. The variable ξ (Eq. (59a)) becomes

$$\xi = 1-\frac{\left(\frac{y}{L}\right)^2}{1-\frac{\omega}{kU_0}} = \overline{\xi}-\frac{\mathrm{i}\varepsilon}{kU_0-\overline{\omega}}\left(\frac{y}{L}\right)^2, \tag{68a}$$

$$\overline{\xi} \equiv 1-\frac{\left(\frac{y}{L}\right)^2}{1-\frac{\overline{\omega}}{kU_0}}, \tag{68b}$$

where $\overline{\xi}$ is calculated for $\omega = \overline{\omega}$, and there is, in addition, a small negative imaginary part. At the critical level $\overline{\xi} = 0$, and $\xi = -\mathrm{i}|\xi|$, justifying the negative phase jump $-\mathrm{i}\pi$ in Eq. (66). The question arises of whether this logarithmic singularity causes

the acoustic pressure P or velocity V to diverge at the critical level. The acoustic pressure equation (65) is given, to leading order equation (64), near the critical level, by

$$P(y_c;k,\omega)=\lim_{\xi\to 0}R_0(\xi)=\lim_{\xi\to 0}\xi^3\log\xi+f_0(0)=f_0(0), \tag{69a}$$

and hence is finite; the transverse acoustic velocity V in Eq. (9), scales on the derivative of the acoustic pressure:

$$P'(y_c;k,\omega)\sim\lim_{\xi\to 0}R'_0(\xi)\left(\frac{\mathrm{d}\xi}{\mathrm{d}y}\right)\sim\lim_{\xi\to 0}\{\xi^2\log\xi+\xi^2+f_1(0)+O(\xi)\}=f_1(0) \tag{69b}$$

is also finite at the critical level (actually zero, see Appendix B). The same applies to longitudinal acoustic velocity, as follows from Eq. (1a). In conclusion, both the acoustic pressure and velocity are finite at the critical level, so the need for a nonlinear theory is not obvious.

Bearing in mind Eqs. (66), the second solution equation (65) in the neighbourhood of the critical level takes the form

$$R_1(\xi)=X(y)-\mathrm{i}\pi W(y), \tag{70a}$$

$$X(y)=\log|y-y_c|W(y)+\sum_{n=0}^{\infty}f_n(0)\left[1-\left(\frac{y}{y_c}\right)^2\right]^n, \tag{70b}$$

where both W (Eq. (64)) and X (Eq. (70b)) are real functions. This pair of solutions is valid for Eq. (71a):

$$1>|\xi|=\left|1-\left(\frac{y}{y_c}\right)^2\right|, \tag{71a}$$

$$0<|y|<y_c\sqrt{2}=L\sqrt{2(1-\Lambda)}\equiv y_*, \tag{71b}$$

in a region excluding the origin, and extending to the wall if $2(1-\Lambda)\geq 1$, i.e. for $\Lambda\leq 1/2$. For $1/2<\Lambda<1$, in order to cover the region near the wall, it is necessary to match the solution equations (64) and (70a) to T (Eq. (56)), S viz:

$$T(y)=B_{11}W(y)+B_{12}\{X(y)-\mathrm{i}\pi W(y)\}, \tag{72a}$$

$$S(y)=B_{21}W(y)+B_{22}\{X(y)-\mathrm{i}\pi W(y)\}, \tag{72b}$$

where some of the constants $B_{11},B_{12},B_{21},B_{22}$ must be complex, since $W,X,T,S(y)$ are all real; one way of making sure that $S(y)$ is real is to take regular expansion point at the wall $y_0=L$ corresponding to $\zeta_0=1/(1-\Lambda)>2$. In this case the solutions $T,S(y)$ are valid (49b) for Eq. (73a):

$$|\zeta_0-\zeta|<\zeta_0,\zeta_0-1, \tag{73a}$$

$$|y|>L\sqrt{\Lambda-1}, \tag{73b}$$

and $\zeta>1$ which implies Eq. (73b); the region equation (73b) overlaps with Eq. (71b) and extends to the wall. For all values of Λ the solutions W,X can be matched to those valid around the axis of the duct:

$$E(y)=C_{11}W(y)+C_{12}X(y), \tag{74a}$$

$$F(y)=C_{21}W(y)+C_{22}X(y), \tag{74b}$$

where the constants $C_{11},C_{12},C_{21},C_{22}$ are real, since all functions $E,F,W,X(y)$ are real. Note that the relation equations (74a), (74b), (72a) and (72b) are valid in disjoint regions, the former $|y|<|y_c|$ including the axis of the duct $y=0$, and the latter $|y|>|y_c|$ including the walls of the duct $|y|=L$.

8. Existence of single or multiple sets of eigenvalues and eigenfunctions

The relation (74a) and (74b) is valid only between the duct axis and the critical level; the right-hand side is valid across the critical level, with $W(y)$ unchanged Eq. (64) and $X(y)$ replaced Eq. (66) by $X(y)-\mathrm{i}\pi W(y)$ in Eq. (70a). Since these solutions extend up to the wall, in the case $0<\Lambda\leq 1/2$, the eigenvalues are determined by

$$0=C_{12}X'(L)+(C_{11}-\mathrm{i}\pi C_{12})W'(L), \tag{75a}$$

$$0=C_{21}X'(L)+(C_{11}-\mathrm{i}\pi C_{22})W'(L), \tag{75b}$$

where $C_{11},C_{12},C_{21},C_{22}$ are real as in Eqs. (74a) and (74b); in the case of $1/2<\lambda<1$ the solution equation (75a) is not valid at the wall, but using Eqs. (72) which is valid, it is possible to arrive (Appendix B) at a formula similar to Eqs. (75). Since the coefficients are real in Eqs. (75) there are four relations:

$$C_{11}W'(L)+C_{12}X'(L)=0=C_{12}W'(L), \tag{76a}$$

$$C_{21}W'(L)+C_{22}X'(L)=0=C_{22}W'(L). \tag{76b}$$

If $C_{12}\neq 0$ or if $C_{22}\neq 0$, then it follows that $W'(L)=0=X'(L)$ vanish simultaneously, which is impossible, since the Wronskian would be zero, and $W(y)$ and $X(y)$ would not be independent solutions. Therefore one must set $C_{12}=0=C_{22}$, in which case Eqs. (74) the pair of solutions $W, X(y)$ about the critical level must be constant multiples of the pair of solutions $E, F(y)$ about the axis:

$$E(y)=C_{11}W(y), \tag{77a}$$

$$F(y)=C_{21}W(y); \tag{77b}$$

these conditions were obtained for $0<\Lambda<1/2$, and for $1/2<\Lambda<1$ one would obtain (Appendix B) from Eqs. (72) similar relations:

$$T(y)=B_{11}W(y), \tag{78a}$$

$$S(y)=B_{21}W(y). \tag{78b}$$

Since E is even in Eq. (77a) and F is odd in Eq. (77b), the two equations imply $C_{11}=0=C_{21}$; similarly Eqs. (78), where $T, S(y)$ are not constant multiples, cannot be satisfied, except if $B_{11}=0=B_{12}$. This shows that there is no single system of real eigenvalues which is valid across the critical levels (in the study of stability of the parabolic shear flow the eigenvalues could be complex, whereas for the acoustic propagation problem they are taken to be real).

In order to explain this, reconsider the wave equation for a general shear flow equation (6) and resume the comparison with the classical self-adjoint operator equation (16). If the wave equation (6) = Eq. (7) is multiplied by a factor $I(y)$:

$$\omega_* IP''-2\omega_*' Ip'+I\omega_*\left(\frac{\omega_*^2}{c^2}-k^2\right)P=0, \tag{79}$$

it coincides with the self-adjoint form equation (16)

$$\lambda\equiv -k^2: \quad GP''+G'P'+(\lambda H-J)P=0, \tag{80}$$

if the following equalities are satisfied:

$$I=\frac{G}{\omega_*}=-\frac{G'}{2\omega_*'}=\frac{H}{\omega_*}=-\frac{Jc^2}{\omega_*^3}; \tag{81}$$

thus G satisfies the differential equation (82a)

$$\frac{G'}{G}=-\frac{2\omega_*'}{\omega_*}, \tag{82a}$$

$$I=\frac{G}{\omega_*}=\omega_*^{-3}, \tag{82b}$$

whose solution is Eq. (17a), and it follows that I is given by Eq. (82b). Using this value of I (Eq. (82b)), then Eq. (81) specifies H, J in agreement with Eqs. (17b) and (17c), which is thus proven; also, substituting Eq. (82b) in Eq. (79) yields the self-adjoint form equation (15) = Eq. (16), i.e.

$$\frac{\mathrm{d}}{\mathrm{d}y}\left[\frac{\mathrm{d}P}{\mathrm{d}y}\frac{1}{\omega-kU(y)}\right]+\left\{\frac{1}{c^2}-\frac{k^2}{[\omega-kU(y)]^2}\right\}P=0. \tag{83}$$

In the case when there is no critical level $\omega>kU(y)$, the coefficients are continuous positive functions of y, as required in Sturm's theorem; however, the eigenvalue $k_n=\sqrt{-\lambda_n}$ appears in several terms, which is not allowed for in Sturm's theorem. One can check, in particular cases, that this does invalidate the theorem. If the theorem were valid, then n-th eigenvalue should correspond to an eigenfunction P_n with n zeros. The plots in Figs. 3–5 of two eigenfunctions for sound in a parabolic shear flow, show at most one zero. Since the boundary condition equations (13) were of Sturm–Liouville type equation (14), and the wave equation (6) in self-adjoint form equation (83) has continuous positive coefficients, the reason for the failure of Sturm's theorem can only be ascribed to the eigenvalues $k_n=\sqrt{-\lambda_n}$ from $\lambda_n=-k_n^2$ in (80) appearing in several coefficients of the wave equation.

The failure of Sturm's theorem in the absence of critical levels, does not augur well for its generalization, allowing for the presence of singularities, viz. Klein's theorem [113]. Although the latter cannot be expected to hold, it might suggest some qualitative features, which would extend to the present case. Klein's oscillation theorem replaces λ by $\lambda+\mu y$ which is not the case in the present problem. It leads to the conclusion that, if the coefficients are positive and continuous in disjoint intervals (a_1,b_1), (a_2,b_2), etc. with $a_1<b_1<a_2<b_2$, then there is a separate set of eigenvalues and eigenfunctions in each interval; in between the intervals, e.g. for (b_1, a_2) nothing is assumed of the coefficients of the differential equation, e.g. they could be discontinuous or have singularities. Although Klein's theorem does not apply to the present problem, the conjecture can be made that a singularity of the wave equation separates two intervals with distinct sets of eigenvalues and eigenfunctions; of course this conjecture cannot be proved by reference to Klein's theorem, whose conditions of validity are not satisfied by the present problem, but evidence may be sought from other directions. It has been shown that there is a single set (Fig. 24) of eigenvalues and eigenfunctions across the duct, in the cases II and III, when there is no critical level. In the case I, when there is

a critical level at the axis of the duct, there is also a single set of eigenvalues; this apparent exception to our conjecture can be discarded, by noting that this is a 'degenerate' critical level, without a logarithmic singularity, and across which all quantities are continuous; it is this sense, an 'apparent' singularity, i.e. singularity of the differential equation in a particular form, which is not a singularity of the solution [120]. By contrast, in case IV, there are two critical levels, with logarithmic singularities, and phase jumps; these are not 'apparent' singularities, which can be made to disappear by a mere change of variable, like in the well-known tidal equation of Laplace [91,121]. In the case IV it has been shown that there is no single set of eigenvalues and eigenfunctions, which is consistent with our conjecture, but does not prove it. Our conjecture is that, in case IV of two critical levels at $y=\pm y_c$, there are (Fig. 25), three sets of eigenfunctions and eigenvalues:

Interval	Eigenvalues	Eigenfunction
$-L<y_1\le y\le y_2<-\lvert y_c\rvert$	k_n^-	S_n , $T_n(y)$
$-\lvert y_c\rvert<y_3\le y\le y_4<\lvert y_c\rvert$	k_n^0	E_n , $F_n(y)$
$\lvert y_c\rvert<y_5\le y\le y_6<1$	k_n^+	S_n , $T_n(y)$

The conjecture must be least partly true, for distinct eigenvalues and eigenfunctions have already been obtained from the solutions E, $F(y)$ in Section 5 and the solutions in Section 6.

9. Impedance walls

When the duct walls are lined, the boundary condition is Eq. (11). In terms of the dimensionless frequency Ω (Eq. (27c)) and specific impedance $\overline{Z}$ defined as

$$\overline{Z}=Z/(\rho c), \tag{84}$$

the boundary condition can be written as

$$\left[P'(y)\mp\frac{\mathrm{i}}{\overline{Z}L}\Omega P(y)\right]_{y=\pm L}=0. \tag{85}$$

Substituting Eq. (18) in Eq. (85) leads to the system of equations:

$$\begin{cases}[C_1E'(L)+C_2F'(L)]-\dfrac{\mathrm{i}\Omega}{\overline{Z}L}[C_1E(L)+C_2F(L)]=0,\\ [-C_1E'(L)+C_2F'(L)]+\dfrac{\mathrm{i}\Omega}{\overline{Z}L}[C_1E(L)-C_2F(L)]=0,\end{cases} \tag{86}$$

where the fact that $E(y)$ and $F'(y)$ are even and $E'(y)$ and $F(y)$ are odd was used. This system leads to

$$\begin{cases}C_2\left[F'(L)-\dfrac{\mathrm{i}\Omega}{\overline{Z}L}F(L)\right]=0,\\ C_1\left[E'(L)-\dfrac{\mathrm{i}\Omega}{\overline{Z}L}E(L)\right]=0.\end{cases} \tag{87}$$

Since the constants C_1 and C_2 cannot vanish simultaneously, the boundary conditions are

$$E'(L)-\frac{\mathrm{i}\Omega}{\overline{Z}L}E(L)=0, \tag{88}$$

$$F'(L)-\frac{\mathrm{i}\Omega}{\overline{Z}L}F(L)=0, \tag{89}$$

for the even and odd functions, respectively. Note that Eqs. (88) and (89) cannot be verified simultaneously, otherwise the Wronskian would vanish at $y=L$. Eqs. (88) and (89) specify the eigenfunctions for the wavenumber K, which can now be complex, for the even or odd modes, respectively. Impedance boundary conditions are illustrated next for a specific impedance $\overline{Z}=1+\mathrm{i}$ and for a dimensionless frequency $\Omega=2.0$. The 'first' eigenvalues obtained for several Mach numbers are presented in Table 10 for even functions E and in Table 11 for odd functions F. The complex values of the wavenumber imply from Eq. (5) stable modes if $\mathrm{Im}(k)>0$ and unstable modes if $\mathrm{Im}(k)<0$. The complex eigenvalues imply that the eigenfunctions are also complex. Figs. 18 and 19 show the modulus and phase of the even and odd eigenfunctions, respectively, for wavevector parallel to the mean flow velocity for several Mach numbers. The modulus and phase of the even and odd eigenfunctions, respectively, are plotted for wavevector anti-parallel to the mean flow velocity for several Mach numbers, for subsonic flow in Figs. 20 and 21 and for supersonic flow in Figs. 22 and 23.

For subsonic mean flow and impedance walls the first eigenfunction increases in amplitude and phase towards the wall (Fig. 18); the first odd eigenfunction (Fig. 19) also increases in amplitude towards the wall but decreases in phase. The amplitude has a maximum at the wall for the odd eigenfunction (Fig. 19), that must vanish on the duct axis $F(0)=0$ and has zero slope at the wall $F'(L)=F'(-L)=0$, and hence is concave downwards; the amplitude of the even eigenfunction (Fig. 18) has zero slope on axis and increases towards the wall, and hence is concave upwards. The subsonic mean flow is considered

Table 10
Eigenvalues $K(\Omega,M)$, as a function of Mach number $M=U_0/c$ on the axis of the duct for dimensionless frequency $\Omega=2.0$ and impedance walls with specific impedance $\overline{Z}=1+\mathrm{i}$, for the even $E_1(y)$ and odd $F_1(y)$ modes, in the case II of horizontal wavevector anti-parallel to the mean flow velocity. For comparison, the first eigenvalues for rigid walls are also shown.

M	Even modes $E(y)$		Odd modes $F(y)$	
	Rigid walls	Impedance walls	Rigid walls	Impedance walls
0.1	−2.14156	−2.36563 − i0.45343	−1.38668	−2.32601 − i0.60015
0.3	−2.49209	−2.70545 − i0.50131	−1.71427	−2.68283 − i0.71208
0.5	−3.02853	−3.17357 − i0.45074	−2.07839	−3.05239 − i0.81542
0.7	−4.30951	−4.34014 − i0.14778	−2.50166	−3.45685 − i0.89636
0.8	−6.26723	−6.27187 − i0.01264	−2.76286	−3.69595 − i0.91945
1.2	−8.83741	−8.83384+i0.00797		
1.5			−7.19973	−7.19325 − i0.06000
1.8	−1.00831	−0.45305+i0.29300	−4.54283	−5.02325+i0.33375
2.0	−0.87457	−0.40579+i0.25860	−2.84041	−1.64269+i0.31699
2.5	−0.66633	−0.32207+i0.20095		

Table 11
Eigenvalues $K(\Omega,M)$, as a function of Mach number $M=U_0/c$ on the axis of the duct for dimensionless frequency $\Omega=2.0$ and impedance walls with specific impedance $\overline{Z}=1+\mathrm{i}$, for the even $E_1(y)$ and odd $F_1(y)$ modes, in the case III of horizontal wavevector parallel to the mean flow velocity. For comparison, the first eigenvalues for rigid walls are also shown.

M	Even modes $E(y)$		Odd modes $F(y)$	
	Rigid walls	Impedance walls	Rigid walls	Impedance walls
0.1	1.87372	2.08190+i0.37733	1.10167	1.16630 − i0.96763
0.3	1.65655	1.83899+i0.30025	0.87143	1.02710 − i0.86061
0.5	1.47623	1.63098+i0.23345	0.69747	0.89740 − i0.74216
0.7			0.57006	0.78228 − i0.63383
0.8			0.51983	0.73114 − i0.58637

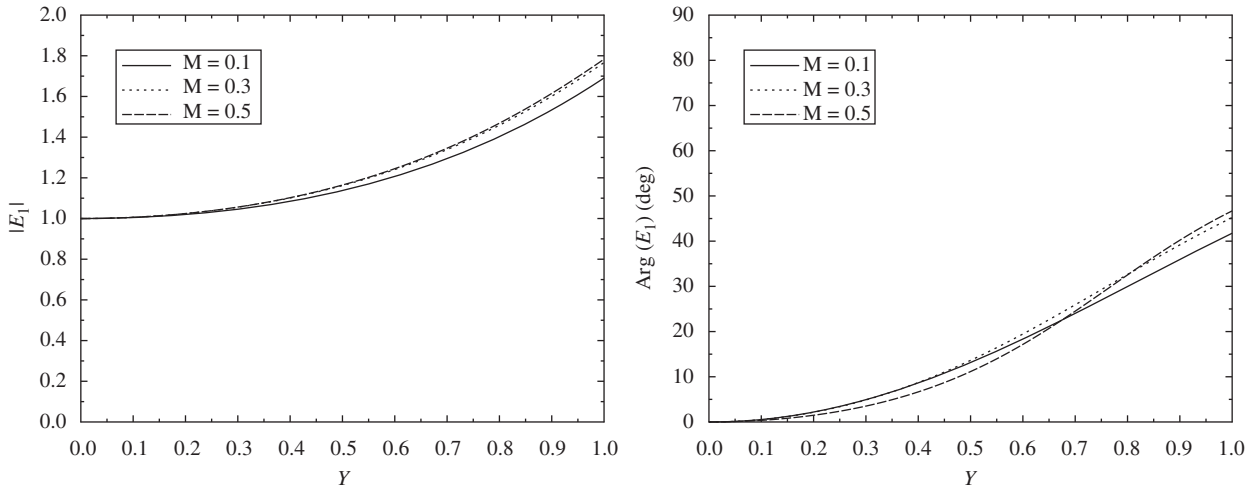

Fig. 18. Even eigenfunction E, as a function of dimensionless distance from axis $Y=y/L$ for fixed dimensionless frequency $\Omega=2.0$, specific impedance $\overline{Z}=1+\mathrm{i}$, and several values of Mach number M, for case III of horizontal wavevector parallel to the mean flow velocity without critical levels in the flow region.

both for the even and odd modes in the case III of horizontal wavevector parallel to the mean flow velocity i.e. downstream propagation (Figs. 18 and 19) and also anti-parallel i.e. upstream propagation (Figs. 20 and 21). In the latter case II of upstream propagation in a subsonic flow the first even eigenfunction (Fig. 20) has amplitude increasing towards the wall at low Mach numbers and decreasing at higher Mach numbers; for the first odd eigenfunction (Fig. 21) the amplitude increases monotonically towards the wall at low Mach numbers, but an inflexion appears at intermediate distance at higher Mach numbers, still subsonic. The phase increases towards the wall both for the first even (Fig. 20) and odd (Fig. 21) eigenfunction

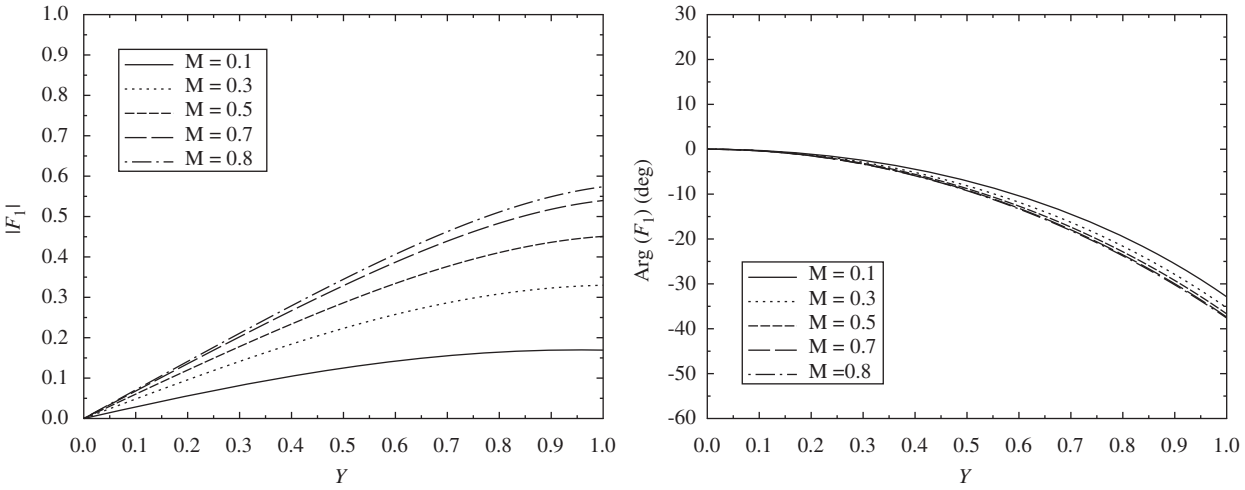

Fig. 19. As Fig. 18, for odd mode *F*.

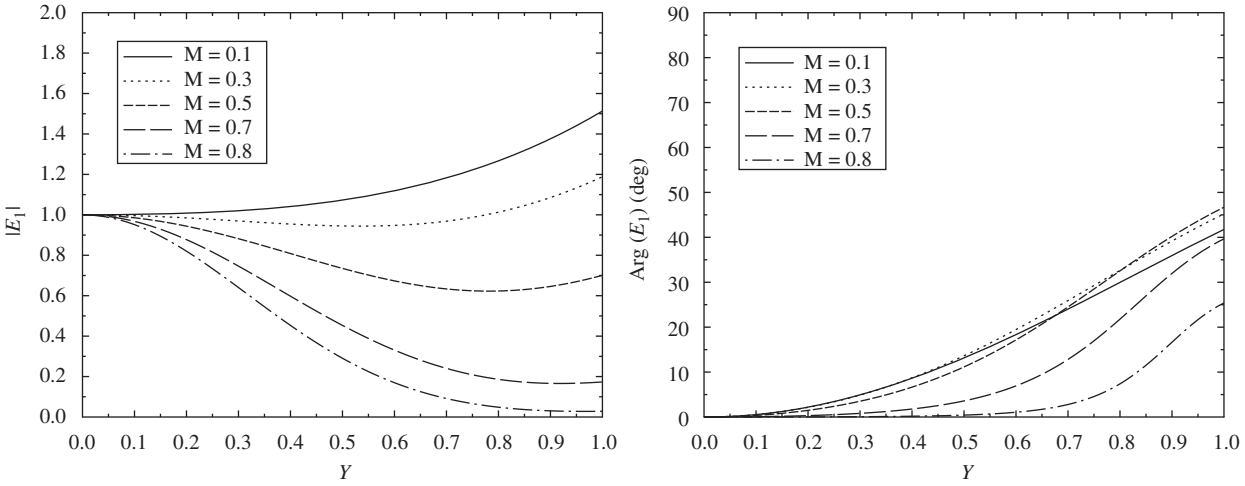

Fig. 20. Even eigenfunction *E*, as a function of dimensionless distance from axis $Y = y/L$ for fixed dimensionless frequency $\Omega = 2.0$, specific impedance $\overline{Z} = 1 + \mathrm{i}$, and several values of subsonic Mach number *M*, for case II of horizontal wavevector anti-parallel to the mean flow velocity without critical levels in the flow region.

for upstream propagation in a subsonic flow. In the case of supersonic flow phase jumps may occur both for the even (Fig. 22) and odd (Fig. 23) eigenfunctions, corresponding to nodes, implying amplitude oscillations.

10. Discussion

The acoustics of shear flows is of considerable importance in connection with the noise of shear layers and boundary layers in free and ducted flows, in applications as diverse as aircraft engines and environmental issues. The practical needs of calculation of the acoustics of shear flows have led to a vast literature concentrating on numerical and approximate analytical solutions. While these serve the basic needs of noise estimation, they do not generally clarify the fundamental mechanisms of interaction between sound and vorticity. The simplest description of the latter is the acoustic wave equation in an unidirectional shear flow, for which only a few exact solutions are known. The most extensively studied case is a linear velocity profile, for which four methods have been used: (i) solution in terms of parabolic cylinder functions [80]; (ii) use of Whittaker functions [81,82]; (iii) the latter may be replaced by confluent hypergeometric functions [83–85]; (iv) separation into even and odd functions relative to the critical level [86]. The linear velocity profile leads to an infinite velocity at infinity; this can be avoided matching to an uniform stream, e.g. to form a boundary layer or shear layer. The 'kink' or angular point of the velocity at the junction(s) of the linear and uniform velocity profiles leads to a discontinuous vorticity in the mean flow, jumping from constant to zero.

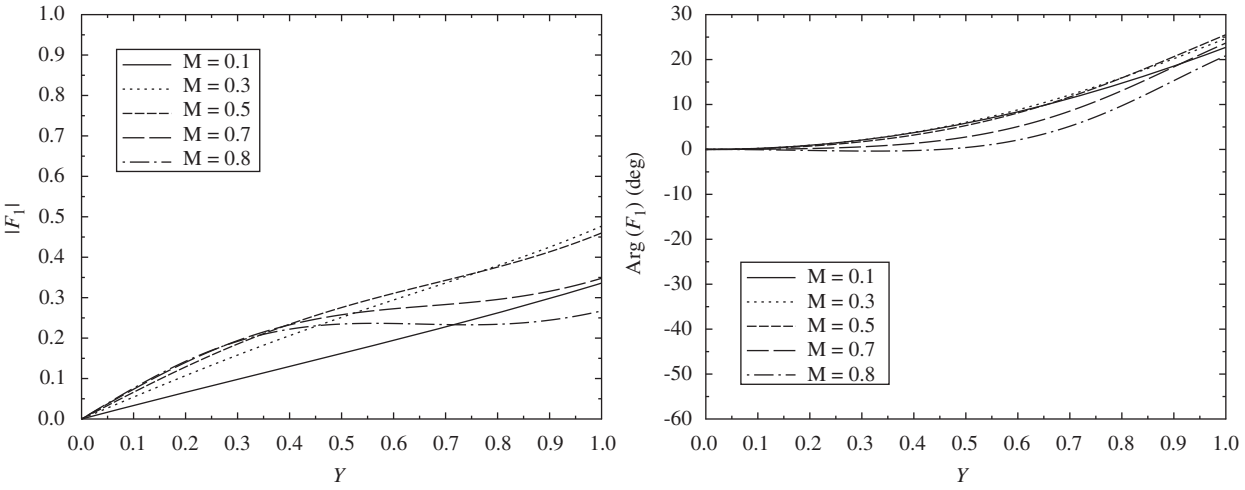

Fig. 21. As Fig. 20, for odd mode *F*.

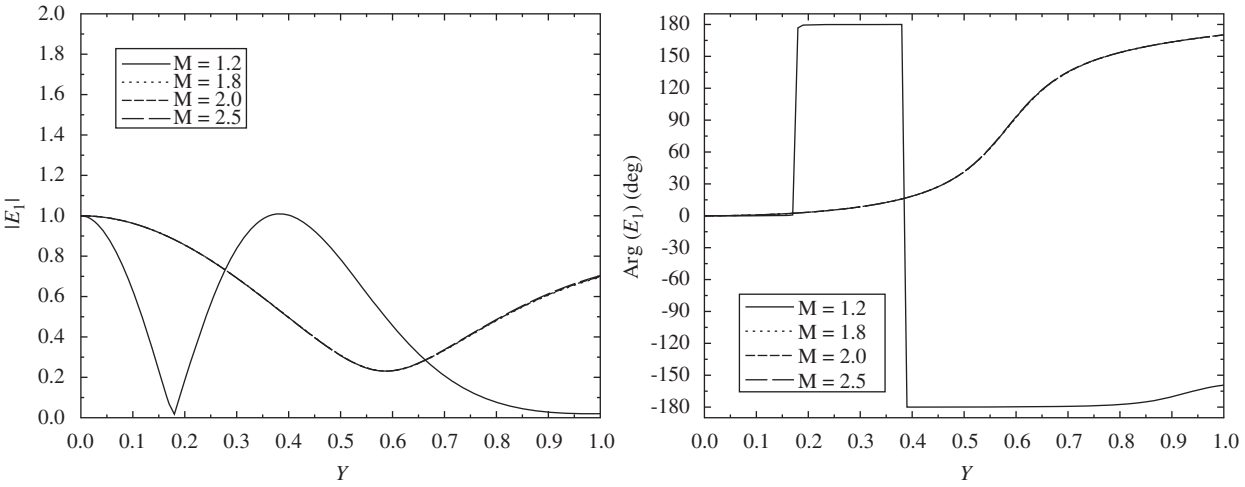

Fig. 22. Even eigenfunction E, as a function of dimensionless distance from axis $Y = y/L$ for fixed dimensionless frequency $\Omega = 2.0$, specific impedance $\overline{Z} = 1 + \mathrm{i}$, and several values of supersonic Mach number M, for case II of horizontal wavevector anti-parallel to the mean flow velocity without critical levels in the flow region. Note that the curves for $M = 1.8$,2.0 and 2.5 are superposed.

The hyperbolic tangent profile leads to a finite velocity at infinity and a smooth vorticity profile decaying to zero at infinity; it has been used to study the acoustics of shear layers [90]. The exponential velocity profile applies to a boundary layer with wall suction [94]; it has been used to study the acoustics of boundary layers [89]. The preceding three cases of exact solution of the acoustic wave equation in a plane unidirectional shear flow assume homentropic conditions; thus temperature, density or sound speed gradients are excluded. An arbitrary temperature profile (and related density and sound speed profiles) transverse to the streamlines is allowed for an isentropic non-homentropic unidirectional shear flow; the case of an homenergetic (i.e. constant stagnation enthalpy) unidirectional shear flow which is non-isothermal, together with a linear velocity profile, appears to be the only exact solution for a non-homentropic flow [87]. It has been extended to include a sound source outside the non-isothermal boundary layer [88]. The present paper presents the fifth case of exact solution of the acoustic wave equation in a shear flow, namely a parabolic flow representing one aspect of acoustics; the latter is the subject of an extensive literature.

The present paper thus concerns the exact solution of the acoustic wave equation in a parabolic shear flow; by exact it is meant that it applies to all frequencies, ranging from the high-frequency ray theory to the low-frequency scattering approximation, including the most significant intermediate case of comparable lengthscales of sound and mean flow, when the acoustic-vortical interaction is strongest. The latter aspect is the main subject of the present paper, and has both well-known and lesser known aspects. The well-known aspects include that the acoustic wave equation in a unidirectional shear flow, together with boundary conditions at the walls of the duct, leads to a boundary-value problem which is not of the Sturm–Liouville type. Thus there is no assurance about that (i) an infinite number of eigenvalues exists and (ii) the

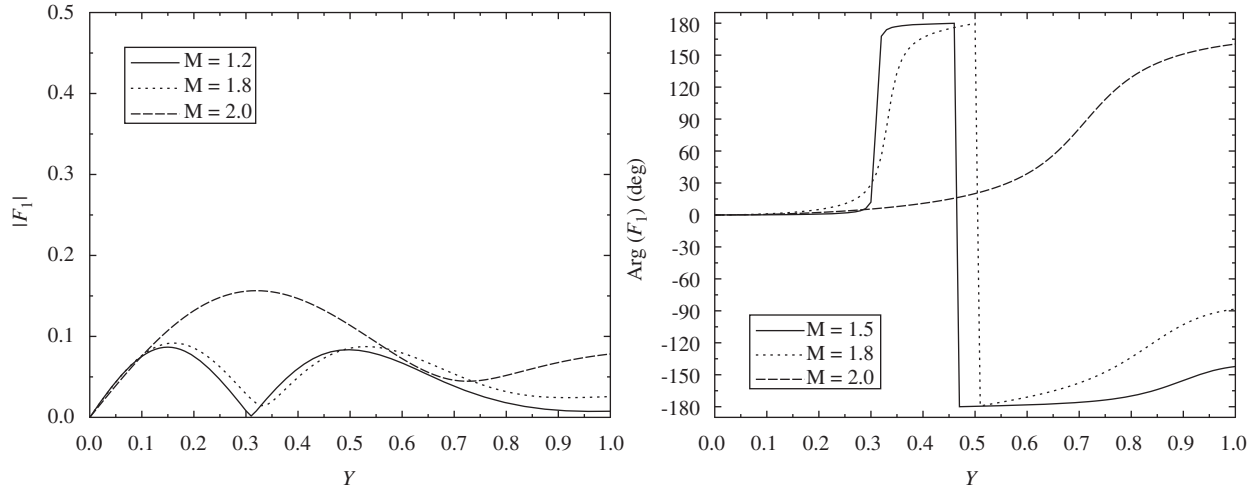

Fig. 23. As Fig. 22, for odd mode *F*.

corresponding eigenfunctions form a complete orthogonal set. It follows that standard modal decomposition methods do not apply. This does not prevent an exact analysis of the acoustics of a parabolic shear flow including boundary conditions at the walls, using the alternative method of series solutions. The latter can be applied at and across the singularities of the wave equation, which are critical levels where the Doppler shifted frequency vanishes, and wave absorption or transformation can occur.

The conclusions of the detailed analysis of the problem for the full range of parameters are not repeated here; they lead to a general conjecture which is worth mentioning: there is no single set of eigenvalues and eigenfunctions for sound is a ducted shear flow with critical levels. The duct is divided by the critical levels into regions with separate sets of eigenvalues and eigenfunctions. The conjecture has been confirmed in all cases considered: (i) if there are no critical levels in the duct (cases II and III in Sections 5 and 6) there is, as usual, a single set of eigenvalues and eigenfunctions (Fig. 24); (ii) if the critical level lies on the axis (case I in Section 4) then by symmetry there must again exist a single set of eigenvalues and eigenfunctions (Fig. 24); (iii) if there are two critical levels in the duct (case IV in Section 5) then (Fig. 25): (a) by symmetry the eigenvalues must be the same in the outer regions near the walls $-L<y<-|y_c|$ and $|y_c|<y<L$; (b) it has been proved (Section 8 and Appendix B) that the eigenvalues must be distinct in the region around the axis $-|y_c|<y<|y_c|$. Since the eigenvalues are the axial wavenumbers k, they are distinct in regions (a) and (b); they are not independent because they are related by the matching of the total wavefield across the critical levels. The matching across the singularities at the critical levels can lead to wave absorption, reflection, or transformation between the different regimes of acoustic propagation.

Appendix A. Logarithmic solution in the neighbourhood of the critical level(s)

Reconsider the solution of the wave equation (60) as a Frobenius–Fuchs series equation (61), in the neighbourhood of the critical layer $\xi=0$ for which the indicial equation (63) has two roots $\sigma=0,3$ differing by an integer. The larger root $\sigma=3$ corresponds to a power series:

$$R_3(\xi)=\sum_{n=0}^{\infty} e_n(3)\xi^{n+3}, \tag{A.1}$$

where the recurrence formula equation (62):

$$\sigma=3:(n+3)ne_n(3)=(n+2)(n-1/2)e_{n-1}(3)+\alpha e_{n-2}(3)-\alpha\beta e_{n-4}(3) \tag{A.2}$$

determines all coefficients $e_n(3)$ with $n=1,2,\ldots$, starting from $e_0(3)$. For the lower root the recurrence formula equation (62):

$$\sigma=0:n(n-3)e_n(0)=(n-1)(n-7/2)e_{n-1}(0)+\alpha e_{n-2}(0)-\alpha\beta e_{n-4}(0), \tag{A.3}$$

applies for $n>3$. For $n=1,2,3$ in both cases hold

$$(\sigma+1)(\sigma-2)e_1(\sigma)=\sigma(\sigma-5/2)e_0(\sigma), \tag{A.4a}$$

$$(\sigma+2)(\sigma-1)e_2(\sigma)=(\sigma+1)\sigma(\sigma-3/2)e_1(\sigma)+\alpha e_0(\sigma), \tag{A.4b}$$

$$(\sigma+3)\sigma e_3(\sigma)=\sigma(\sigma+2)(\sigma-1/2)e_2(\sigma)+\alpha e_1(\sigma). \tag{A.4c}$$

For $\sigma=0$ then $e_1(\sigma)=0$ by Eq. (A.4a), so $e_2(\sigma)$ depends only on $e_0(\sigma)$ by Eq. (A.4b). Also $e_3(\sigma)$ is arbitrary in Eq. (A.4c). Thus the second solution:

$$\overline{g}_0(\xi)=\sum_{n=0}^{\infty}e_n(0)\xi^n=\sum_{n=3}^{\infty}e_n(0)\xi^n=\sum_{n=0}^{\infty}e_{n+3}(0)\xi^{n+3}=g_4(\xi), \tag{A.5}$$

coincides with Eq. (A.1), since $e_{n+3}(0)=e_n(3)$; the latter relation follows noting that the substitution $n\to n+3$ transforms Eq. (A.3) to Eq. (A.2). Thus the two solutions coincide, and a new linearly independent solution is needed.

To obtain the latter, note that, if the recurrence relation Eq. (62) is satisfied, and Eq. (61) is substituted in the differential equation (60), one obtains

$$(1-\xi)\xi R''+(\tfrac{3}{2}\xi-2)R'+\alpha\xi(\xi^2\beta-1)R=j(\sigma), \tag{A.6}$$

where

$$j(\sigma)\equiv\sigma(\sigma-3)e_0; \tag{A.7}$$

thus the differential equation (60) is satisfied by Eq. (A.6) provided that $j(\sigma)=0$ i.e. $\sigma=0,3$, which gives the solutions R_3, R_0. If e_0 is replaced by $e_0=C\sigma$ then Eq. (A.7) is replaced by

$$j(\sigma)=C\sigma^2(\sigma-3); \tag{A.8}$$

the differential equation (60) is satisfied by $R_\sigma(\xi)$ with $\sigma=0,3$ i.e. the coincident solutions and $R_3=R_0$ (Eq. (A.5)), and also by a new solution:

$$\overline{R}_0(\xi)=\lim_{\sigma\to 0}\frac{\partial}{\partial\sigma}\{R_\sigma(\xi)\} \tag{A.9}$$

Recalling Eq. (61), viz.:

$$\overline{R}_0(\xi)=\lim_{\sigma\to 0}\frac{\partial}{\partial\sigma}\sum_{n=0}^{\infty}e_n(\sigma)\xi^{n+\sigma}=\log\xi\sum_{n=1}^{\infty}e_n(0)\xi^n+\sum_{n=0}^{\infty}e_n'(0)\xi^n, \tag{A.10}$$

it follows that this solution is linearly independent from the preceding.

The solution equation (A.10) consists

$$\overline{R}_0(\xi)=R_3(\xi)\log\xi+R_*(\xi) \tag{A.11}$$

of Eq. (A.1) multiplied by a logarithm, and adds a series equation (A.12a):

$$R_*(\xi)=\sum_{n=1}^{\infty}f_n(0)\xi^n, \tag{A.12a}$$

$$f_n(\sigma)=e_n'(\sigma), \tag{A.12b}$$

with coefficients equation (A.12b). The solution equations (A.11), (A.12a) coincide with Eq. (65), and has coefficients $f_n(0)$; the first of these can be obtained from Eqs. (A.4b) and (A.4c) with $e_0=C\sigma$ by using Eqs. (A.12b), viz:

$$f_0(0)=C, \tag{A.13a}$$

$$f_1(0)=0, \tag{A.13b}$$

$$f_2(0)=-\alpha C/2, \tag{A.13c}$$

$$f_3(0)=-\frac{e_3(0)}{3}-\frac{f_2(0)}{3}=\frac{2\alpha C}{9}. \tag{A.13d}$$

Differentiating Eq. (62) with regard to σ leads to

$$(n+\sigma)(n+\sigma+3)e_n'(\sigma)=(n+\sigma-1)(n+\sigma-7/2)e_{n-1}'(\sigma)+\alpha e_{n-2}'(\sigma)-\alpha\beta e_{n-4}'(\sigma)-(2n+2\sigma+3)e_n(\sigma)+(2n+2\sigma-9/2)e_{n-1}(\sigma); \tag{A.14}$$

setting $\sigma=0$ specifies the recurrence relation for $f_n(0)$, viz.:

$$n(n+3)f_n=(n-1)(n-7/2)f_{n-1}+\alpha f_{n-2}-\alpha\beta f_{n-4}-(2n+3)e_n+(2n-9/2)e_{n-1}. \tag{A.15}$$

This completes the specification of the complementary function equation (A.12a), and specifies Eqs. (69a) the acoustic pressure and velocity at the critical level, viz. the former is finite and non-zero equation (A.13a), and the latter is zero equation (A.13b).

Appendix B. Relation between the three pairs of solutions and separation of sets of eigenfunctions and eigenvalues by critical levels

The critical levels lie in the duct for $0 < \Lambda < 1$, and in the case $0 < \Lambda \leq 1/2$ the whole flow region can be covered with two pairs of solutions. Using these, it was shown in Section 8 that there is not a single set of eigenvalues and eigenfunctions covering the whole duct, as in Fig. 24; instead, as in Fig. 25, there are three sets of eigenvalues and eigenfunctions, in three regions separated by the critical levels and the walls. These conclusions hold whenever the critical levels exist, i.e. also for $1/2 < \Lambda < 1$. In the latter case the three pairs of solutions are needed to construct the eigenvalues and eigenfunctions in each region; also, the statement that there is no single set of eigenvalues and eigenfunctions covering the whole duct, also applies in this case. The proof, which is given in the sequel, is somewhat more involved than in Section 8, because the three (instead of two) pairs of solutions have to be used.

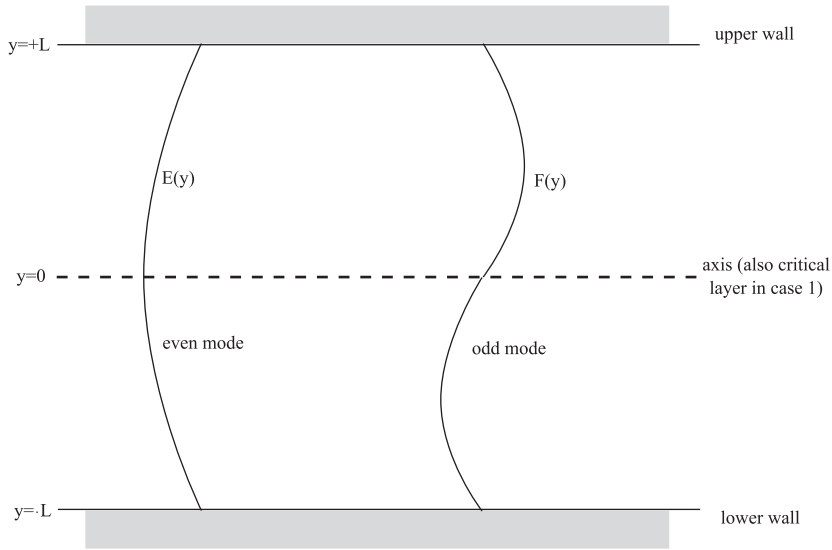

Fig. 24. Single system of eigenvalues, for even E and odd F eigenfunctions, valid across the whole duct, when there is no critical level, or only one critical level exists on the axis.

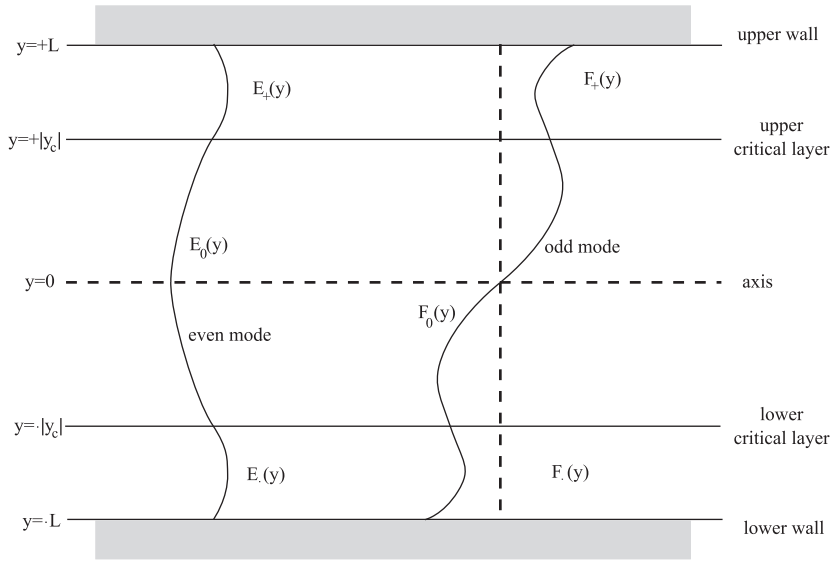

Fig. 25. Conjecture that, if two critical levels are present, there may be a distinct set of eigenvalues and eigenfunctions E, F in three regions: E_0, F_0 between the critical levels $y = \pm |y_c|$, and $E_\pm$, $F_\pm$ between the critical levels and the walls $y = \pm L$.

A linearly independent pair of solutions is specified: (i) in $0 \leq |y| \leq \|y_c|$ by Eqs. (74); (ii) using Eqs. (66) and (70a) yields

$$\begin{bmatrix} E(y) \\ F(y) \end{bmatrix} = \begin{bmatrix} C_{12} & (C_{11} - \mathrm{i}\pi C_{12}) \\ C_{22} & (C_{21} - \mathrm{i}\pi C_{22}) \end{bmatrix} \begin{bmatrix} X(y) \\ W(y) \end{bmatrix}, \tag{B.1}$$

for $|y_c| < |y| < y_*$ in Eq. (71b); (iii) Eqs. (72) gives

$$\begin{bmatrix} E(y) \\ F(y) \end{bmatrix} = \begin{bmatrix} C_{12} & (C_{11} - \mathrm{i}\pi C_{12}) \\ C_{22} & (C_{21} - \mathrm{i}\pi C_{22}) \end{bmatrix} \begin{bmatrix} B_{12} & (B_{11} - \mathrm{i}\pi B_{12}) \\ B_{22} & (B_{21} - \mathrm{i}\pi B_{22}) \end{bmatrix}^{-1} \begin{bmatrix} T(y) \\ S(y) \end{bmatrix}, \tag{B.2}$$

for $|y_*| < |y| < |y_{**}| > L$. The latter solution applies at the walls $y = \pm L$, so that the boundary conditions can be applied, e.g. hard-wall boundary conditions:

$$0 = \begin{bmatrix} E'(L) \\ F'(L) \end{bmatrix} = \begin{bmatrix} C_{12} & (C_{11} - \mathrm{i}\pi C_{12}) \\ C_{22} & (C_{21} - \mathrm{i}\pi C_{22}) \end{bmatrix} \begin{bmatrix} B_{12} & (B_{11} - \mathrm{i}\pi B_{12}) \\ B_{22} & (B_{21} - \mathrm{i}\pi B_{22}) \end{bmatrix}^{-1} \begin{bmatrix} T'(L) \\ S'(L) \end{bmatrix}. \tag{B.3}$$

Note that, because the system equations (72) are invertible, the inverse B-matrix in Eqs. (B.2) and (B.3) exists.

Noting that the order of the product of two matrices can be inverted, if all matrices are transposed, the system equation (B.3) becomes

$$0 = \begin{bmatrix} B_{12} & B_{22} \\ (B_{11} - \mathrm{i}\pi B_{12}) & (B_{21} - \mathrm{i}\pi B_{22}) \end{bmatrix}^{-1} \begin{bmatrix} C_{12} & C_{22} \\ (C_{11} - \mathrm{i}\pi C_{12}) & (C_{21} - \mathrm{i}\pi C_{22}) \end{bmatrix} \begin{bmatrix} S'(L) \\ T'(L) \end{bmatrix}. \tag{B.4}$$

Since the B-matrix has an inverse, the transpose B-matrix also has inverse, and multiplying by the latter, Eq. (B.4) becomes

$$\begin{bmatrix} C_{12} & C_{22} \\ (C_{11} - \mathrm{i}\pi C_{12}) & (C_{21} - \mathrm{i}\pi C_{22}) \end{bmatrix} \begin{bmatrix} S'(L) \\ T'(L) \end{bmatrix} = 0, \tag{B.5}$$

where the C_{11}, C_{12}, C_{21}, C_{22} come from Eqs. (74) and are all real:

$$C_{12} S'(L) + C_{22} T'(L) = 0 = C_{11} S'(L) + C_{21} T'(L). \tag{B.6}$$

Now $S'(L) = 0 = T'(L)$ cannot vanish simultaneously, otherwise the Wronskian of S, $T(y)$ would vanish, and they would not be linearly independent solutions. Thus one has

$$C_{12} C_{21} = C_{11} C_{22} \tag{B.7}$$

implying that Eqs. (74) is not invertible. Thus a contradiction has been obtained, which is that there is no single set of eigenvalues and eigenfunctions covering the whole flow region. The preceding proof assumes real wavenumber and hard walls. It could be invalidated for complex wavenumbers, associated with impedance walls or a stability study. For a real wavenumber, it possible to specify sets of eigenvalues and eigenfunctions in regions separated by critical levels, viz. using Eqs. (74) for $|y| < |y_c|$, and Eqs. (72) in $|y| > |y_c|$. The conclusion could be quite different in the framework of stability analysis, [101,102] in which the frequency is taken to be complex, allowing temporal growth or decay.

References

[1] M.E. Goldstein, *Aeroacoustics*, McGraw-Hill, 1976.
[2] D.G. Crighton, Acoustics as a branch of fluid mechanics, *Journal of Fluid Mechanics* 106 (1981) 261–298.
[3] A.P. Dowling, J.E.F. Williams, *Sound and Sources of Sound*, Ellis Horwood Limited, 1983.
[4] W.K. Blake, *Mechanics of Flow-Induced Sound and Vibration*, Academic Press, 1986, (2 vols.).
[5] L.M.B.C. Campos, On waves in gases. Part I: Acoustics of jets, turbulence, and ducts, *Reviews of Modern Physics* 58 (1) (1986) 117–182.
[6] L.M.B.C. Campos, On the spectra of aerodynamic noise and aeroacoustic fatigue, *Progress in Aerospace Sciences* 33 (1997) 353–389.
[7] L.M.B.C. Campos, On some recent advances in aeroacoustics, *International Journal of Sound and Vibration* 11 (2005) 27–45.
[8] L.M.B.C. Campos, On 36 forms of the acoustic wave equation in potential flows and inhomogeneous media, *Applied Mechanics Reviews* 60 (4) (2007) 149–171.
[9] G. Raman, *Jet Aeroacoustics*, Multi Science Publishing, 2008.
[10] L.M.B.C. Campos, W. Schroder, Combustion noise, *International Journal of Aeroacoustics* 8 (2009) 1–176.
[11] E.W. Graham, B.B. Graham, Effect of a shear layer on plane waves of sound in a fluid, *Journal of the Acoustical Society of America* 46 (1) (1969) 169–175.
[12] T. Balsa, The far-field of high-frequency convected, singularities in shear flows with application to jet noise prediction, *Journal of Fluid Mechanics* 74 (1976) 193–208.
[13] T. Balsa, Refraction and shielding of sound from a source in a jet, *Journal of Fluid Mechanics* 76 (1976) 443–456.
[14] L.M.B.C. Campos, The spectral broadening of sound in turbulent shear layers. Part 1: the transmission of sound through turbulent shear layers, *Journal of Fluid Mechanics* 89 (1978) 723–749.
[15] L.M.B.C. Campos, The spectral broadening of sound in turbulent shear layers. Part 2: the spectral broadening of sound and aircraft noise, *Journal of Fluid Mechanics* 89 (1978) 751–783.
[16] M.E. Goldstein, Scattering and distortion of the unsteady motion on transversely sheared mean flows, *Journal of Fluid Mechanics* 91 (4) (1979) 601–632.
[17] M.E. Goldstein, High frequency sound emission from moving point multipole sources embedded in arbitrary transversely sheared mean flows, *Journal of Sound and Vibration* 80 (4) (1982) 499–522.
[18] M.E. Goldstein, S.J. Leib, The aeroacoustics of slowly diverging supersonic jets, *Journal of Fluid Mechanics* 600 (2008) 291–337.
[19] C.K.W. Tam, K. Viswanathan, K.K. Ahuja, J. Panda, The sources of jet noise: experimental evidence, *Journal of Fluid Mechanics* 615 (2008) 253–292.
[20] D.J. Bodony, S.K. Lele, Low frequency sound sources in high-speed turbulent jets, *Journal of Fluid Mechanics* 617 (2008) 231–253.

[21] M.K. Myers, S.L. Chuang, Uniform asymptotic approximations for duct acoustic modes in a thin boundary-layer flow, *AIAA Journal* 22 (1983) 1234–1241.
[22] D.B. Hanson, Shielding of prop-fan cabin noise by the fuselage boundary-layer, *Journal of Sound and Vibration* 92 (4) (1984) 591–598.
[23] L.M.B.C. Campos, Effects on acoustic fatigue loads of multiple reflection between a plate and a turbulent wake, *Acustica* 76 (1992) 109–117.
[24] L.M.B.C. Campos, On the correlation of acoustic pressures induced by a turbulent wake on a nearby wall, *Acustica* 82 (1) (1996) 9–17.
[25] L.M.B.C. Campos, A. Bourgine, B. Bonomi, Comparison of theory and experiment on aeroacoustic loads and deflections, *Journal of Fluids and Structures* 13 (1) (1999) 3–35.
[26] B. Liu, Noise radiation of aircraft panels subjected to boundary layer pressure fluctuations, *Journal of Sound and Vibration* 314 (3–5) (2008) 693–711.
[27] S. Park, G.C. Lauchle, Wall pressure fluctuation spectra due to boundary-layer transition, *Journal of Sound and Vibration* 319 (3–5) (2009) 1067–1082.
[28] E. Dokumaci, On attenuation of plane sound waves in turbulent mean flow, *Journal of Sound and Vibration* 320 (4–5) (2009) 1131–1136.
[29] D.H. Tack, R.F. Lambert, Influence of shear flow on sound attenuation in lined ducts, *Journal of the Acoustical Society of America* 38 (1965) 655–666.
[30] P. Mungur, G.M.L. Gladwell, Acoustic wave propagation in a shear flow contained in a duct, *Journal of Sound and Vibration* 9 (1) (1969) 28–48.
[31] P. Mungur, H.E. Plumblee, Propagation and attenuation of sound in a soft-walled annular duct containing a sheared flow, SP 207, NASA, 1969.
[32] A.S. Hersh, I. Catton, Effect of shear flow on sound propagation in rectangular ducts, *Journal of the Acoustical Society of America* 50 (3) (1970) 992–1003.
[33] S. Mariano, Effect of wall shear layers on the sound attenuation in acoustically lined rectangular ducts, *Journal of Sound and Vibrations* 19 (1971) 261–275.
[34] W. Eversman, Effect of boundary layer on the transmission and attenuation of sound in an acoustically treated circular duct, *Journal of the Acoustical Society of America* 49 (5) (1970) 1372–1380.
[35] P.N. Shankar, On acoustic refraction by duct shear layers, *Journal of Fluid Mechanics* 47 (1971) 81–91.
[36] P.N. Shankar, Acoustic reffraction and attenuation in cylindrical and annular ducts, *Journal of Sound and Vibration* 22 (1972) 233–296.
[37] P.N. Shankar, Sound propagation in shear layers, *Journal of Sound and Vibration* 40 (1972) 51–76.
[38] S.-H. Ko, Sound attenuation in lined rectangular ducts with flow and its application to the reduction of aircraft engine noise, *Journal of the Acoustical Society of America* 50 (6) (1971) 1418–1432.
[39] W. Eversman, R.J. Beckemeyer, Transmission of sound in ducts with thin shear layers—convergence to the uniform case, *Journal of the Acoustical Society of America* 52 (1) (1972) 216–220.
[40] A.H. Nayfeh, J.E. Kaiser, D.P. Telionis, Acoustics of aircraft engine-duct systems, *AIAA Journal* 13 (2) (1975) 130–153.
[41] M.A. Swinbanks, The sound field generated by a source distribution in a long duct carrying sheared flow, *Journal of Sound and Vibration* 40 (1) (1975) 51–76.
[42] R. Mani, Sound propagation in parallel sheared flows in ducts: the mode estimation problem, *Proceedings of the Royal Society of London Series A* 371 (1980) 393–412.
[43] S. Ishii, T. Kakutani, Acoustic waves in parallel shear flows in a duct, *Journal of Sound and Vibration* 113 (1) (1987) 127–139.
[44] G.G. Vilenski, S.W. Rienstra, On hydrodynamic and acoustic modes in a ducted shear flow with wall lining, *Journal of Fluid Mechanics* 583 (2007) 45–70.
[45] G.G. Vilenski, S.W. Rienstra, Numerical study of acoustic modes in ducted shear flow, *Journal of Sound and Vibration* 307 (2007) 610–626.
[46] Y. Aurégan, M. Leroux, Experimental evidence of an instability over an impedance wall in a duct with flow, *Journal of Sound and Vibration* 317 (2008) 432–439.
[47] E.J. Brambley, N. Peake, Sound transmission in strongly curved slowly varying cylindrical ducts with flow, *Journal of Fluid Mechanics* 596 (2008) 387–412.
[48] S. Rienstra, B.J. Tester, An analytic Green's function for a lined circular duct containing uniform mean flow, *Journal of Sound and Vibration* 317 (3–5) (2008) 994–1016.
[49] B. Veitch, N. Peake, Acoustic propagation and scattering in the exhaust flow from coaxial cylinders, *Journal of Fluid Mechanics* 613 (2008) 275–307.
[50] M. Knutsson, M. Åbom, Sound propagation in narrow tubes including effects of viscothermal and turbulent damping with application to charge air coolers, *Journal of Sound and Vibration* 320 (2009) 289–321.
[51] F. Silva, P. Guillemaina, J. Kergomard, B. Mallaronia, A. Norris, Approximation formulae for the acoustic radiation impedance of a cylindrical pipe, *Journal of Sound and Vibration* 322 (1–2) (2009) 255–263.
[52] E.J. Brambley, Fundamental problems with the model of uniform flow over acoustic linings, *Journal of Sound and Vibration* 322 (2009) 1026–1037.
[53] R.F. Salant, Symmetric normal modes in a uniformly rotating fluid, *The Journal of the Acoustical Society of America* 43 (1968) 1302–1305.
[54] M.S. Howe, The generation of sound by vorticity wave in swirling flows, *Journal of Fluid Mechanics* 81 (1977) 369–383.
[55] J.L. Kerrebrock, Small disturbances in turbomachine annuli with swirl, *AIAA Journal* 15 (1977) 794–803.
[56] E.M. Greitzer, T. Strand, Axysymmetric swirling flows in turbomachinery annuli, *Journal of Engineering for Power* 100 (1978) 618–629.
[57] V.V. Golubev, H.M. Atassi, Sound propagation in an annular duct mean potential flow, *Journal of Sound and Vibration* 198 (1996) 601–606.
[58] V.V. Golubev, H.M. Atassi, Acoustic vorticity waves in swirling flows, *Journal of Sound and Vibration* 209 (2) (1998) 203–222.
[59] C.K.W. Tam, L. Auriault, The wave modes in ducted swirling flows, *Journal of Fluid Mechanics* 371 (1998) 1–20.
[60] A. Cooper, N. Peake, Trapped acoustics modes in aeroengine intakes with swirling flow, *Journal of Fluid Mechanics* 419 (2000) 151–175.
[61] A.J. Cooper, N. Peake, Propagation of unsteady disturbances in slowly varying duct with swirling mean flow, *Journal of Fluid Mechanics* 445 (2001) 207–234.
[62] L.M.B.C. Campos, P.G.T.A. Serrão, On the acoustics of unbounded and ducted vortex flows, *SIAM Journal of Applied Mathematics* 65 (2004) 1353–1368.
[63] A.J. Cooper, N. Peake, Upstream-radiated rotor–stator interaction noise in mean swirling flow, *Journal of Fluid Mechanics* 523 (2005) 219–250.
[64] C.J. Heaton, N. Peake, Acoustic scattering in a duct with mean swirling flow, *Journal of Fluid Mechanics* 540 (2005) 189–220.
[65] C.J. Heaton, N. Peake, Algebraic and exponential instability in inviscid swirling flow, *Journal of Fluid Mechanics* 565 (2006) 279–318.
[66] L.M.B.C. Campos, On 24 forms of the accoustic wave equation in vortical flows and dissipative media, *Applied Mechanics Reviews* 60 (6) (2007) 291–315.
[67] M.S. Howe, Multiple scattering of sound by turbulence and other inhomogeneities, *Journal of Sound and Vibration* 27 (4) (1973) 455–479.
[68] M. J. Lighthill, On the energy scattered from the interaction of turbulence with sound and shock waves, *Proceeding of the Cambridge Philosophical Society*44 (1953) 531–551.
[69] P.O.A.L. Davies, M.J. Fisher, M.J. Barrat, The characteristics of the turbulence in the mixing region of a round jet, *Journal of Fluid Mechanics* 15 (3) (1963) 337–367.
[70] D.W. Schmidt, P.M. Tilmann, Experimental study of sound-wave phase fluctuations caused by turbulent wakes, *The Journal of the Acoustical Society of America* 47 (1970) 1310–1322.
[71] C.M. Ho, L.S.G. Kovasznay, Acoustical shadowgraph, *Physics of Fluids* 19 (1976) 1118–1123.
[72] R.M. Munt, Acoustic radiation from a semi-infinite circular duct in an uniform subsonic mean flow, *Journal of Fluid Mechanics* 83 (1977) 609–640.
[73] L.M.B.C. Campos, Modern trends in research on waves in fluids. Part I: generation and scattering by turbulent and inhomogeneous flows, *Portugaliæ Physica* 14 (3–4) (1983) 121–143.
[74] L.M.B.C. Campos, C.M. Macedo, On the prediction of the broadband noise of helicopter rotors from the impulsive component, *Journal d'Acoustique* 5 (1992) 531–542.
[75] L.M.B.C. Campos, P.G.T.A. Serrão, On the directivity and spectra of noise from unheated and heated jets, *International Journal of Aeroacoustics* 6 (2) (2007) 93–126.
[76] B. Haurwitz, Zur Theorie der Wellenbewegungen in Luft und Wasser, Veroffs, *Geophysical Institute of Leipzig* 6 (1931) 324–364.
[77] D. Kucheman, Storungsbewegungen in einer Gasstromung mit Grenzschicht, *Zeitschrift für Angewandte Mathematik und Mechanik* 18 (1938) 207–222.
[78] D.C. Pridmore-Brown, Sound propagation in a fluid flowing through an attenuating duct, *Journal of Fluid Mechanics* 4 (1958) 393–406.
[79] W. Möhring, E.-A. Müller, F. Obermeier, Problems in flow acoustics, *Reviews of Modern Physics* 55 (3) (1983) 707–724.

[80] M.E. Goldstein, E. Rice, Effect of shear on duct wall impedance, *Journal of Sound and Vibration* 30 (1) (1973) 79–84.
[81] D.S. Jones, The scattering of sound by a simple shear layer, *Proceedings of the Royal Society of London, Series A* 284 (1977) 287–328.
[82] D.S. Jones, Acoustics of a splitter plate, *Journal of the Institute of Mathematics and its Applications* 21 (1978) 197–209 verificar revista, etc..
[83] J.N. Scott, Propagation of sound waves through a linear shear layer, *AIAA Journal* 17 (3) (1979) 237–244.
[84] S.P. Koutsoyannis, Characterization of acoustic disturbances in linearly sheared flows, *Journal of Sound and Vibration* 68 (2) (1980) 187–202.
[85] S.P. Koutsoyannis, K. Karamcheti, D.C. Galant, Acoustic resonances and sound scattering by a shear layer, *AIAA Journal* 18 (12) (1980) 1446–1454.
[86] L.M.B.C. Campos, J.M.G.S. Oliveira, M.H. Kobayashi, On sound propagation in a linear flow, *Journal of Sound and Vibration* 219 (5) (1999) 739–770.
[87] L.M.B.C. Campos, M.H. Kobayashi, On the propagation of sound in a high-speed non-isothermal shear flow, *International Journal of Aeroacoustics* 8 (3) (2009) 199–230.
[88] L.M.B.C. Campos, M.H. Kobayashi, On sound transmission from a source outside a non-isothermal boundary-layer, *AIAA Journal* 48 (5) (2010) 878–892.
[89] L.M.B.C. Campos, P.G.T.A. Serrão, On the acoustics of an exponential boundary layer, *Philosophical Transactions of the Royal Society of London, Series A* 356 (1998) 2335–2378.
[90] L.M.B.C. Campos, M.H. Kobayashi, On the reflection and transmission of sound in a thick shear layer, *Journal of Fluid Mechanics* 420 (2000) 1–24.
[91] H. Lamb, *Hydrodynamics*, Cambridge University Press, 1932.
[92] L.D. Landau, E.F. Lifshitz, *Fluid Dynamics*, Pergamon, 1953.
[93] G.B. Whitham, *Linear and Non-linear Waves*, Wiley, 1974.
[94] H. Schlichting, *Boundary-Layer Theory*, sixth ed., McGraw-Hill, 1968.
[95] F.P. Bretherton, Propagation in slowly varying waveguides, *Proceedings of the Royal Society of London. Series A, Mathematical and Physical Sciences* 302 (1968) 555–576.
[96] M.J. Lighthill, *Waves in Fluids*, Cambridge University Press, 1978.
[97] L.M.B.C. Campos, On waves in gases. Part II: interaction of sound with magnetic and internal modes, *Reviews of Modern Physics* 59 (1) (1987) 363–462.
[98] L.M.B.C. Campos, On hydromagnetic waves in atmospheres with application to the sun, *Theoretical and Computational Fluid Dynamics* 10 (1–4) (1998) 37–70.
[99] J.R. Booker, F.P. Bretherton, The critical layer for internal gravity waves in a shear flow, *Journal of Fluid Mechanics* 27 (3) (1967) 513–539.
[100] H.P. Greenspan, *Theory of Rotating Fluids*, Cambridge University Press, 1968.
[101] C.C. Lin, *Hydrodynamic Stability*, Oxford University Press, 1944.
[102] P.G. Drazin, W.H. Reid, *Hydrodynamic Stability*, Cambridge University Press, 1981.
[103] J.F. McKenzie, On the existence of critical levels, with applications to hydromagnetic waves, *Journal of Fluid Mechanics* 58 (4) (1973) 709–726.
[104] L.M.B.C. Campos, On the properties of hydromagnetic-waves in the vicinity of critical levels and transition layers, *Geophysical and Astrophysical Fluid Dynamics* 40 (1–2) (1988) 93–132.
[105] M. Yanowitch, Effect of viscosity on vertical oscillations of an isothermal atmosphere, *Canadian Journal of Physics* 45 (6) (1967) 2003–2008.
[106] L.M.B.C. Campos, On viscous and resistive dissipation of hydrodynamic and hydromagnetic-waves in atmospheres, *Journal de Mecanique Theorique et Appliquee* 2 (6) (1983) 861–891.
[107] P. Lyons, M. Yanowitch, Vertical oscillations in a viscous and thermally conducting isothermal atmosphere, *Journal of Fluid Mechanics* 66 (2) (1974) 273–288.
[108] L.M.B.C. Campos, P.M.V.M. Mendes, On dissipative Alfven waves in atmospheres with steep temperature gradients, *Geophysical and Astrophysical Fluid Dynamics* 91 (1–2) (1999) 103–130.
[109] L.M.B.C. Campos, On 3-dimensional acoustic-gravity waves in model non-isothermal atmospheres, *Wave Motion* 5 (1) (1983) 1–14.
[110] P.S. Cally, Magnetohydrodynamic critical levels and radiative damping, *Astronomy and Astrophysics* 136 (1984) 121–126.
[111] L.M.B.C. Campos, Comparison of exact-solutions and the phase mixing approximation for dissipative Alfven waves, *European Journal of Mechanics B—Fluids* 12 (2) (1993) 187–216.
[112] L.M.B.C. Campos, N.L. Isaeva, P.J.S. Gil, On Kolmogorov- and Kraichnan-type spectra due to the reflection alfven waves, *Physics of Plasmas* 6 (7) (1999) 2870–2882.
[113] E.L. Ince, *Ordinary Differential Equations*, Dover, New York, 1926, 1956.
[114] L.M.B.C. Campos, On singularities and solutions of the extended hypergeometric differential equation, *Integral Transforms and Special Functions* 9 (2) (2000) 99–120.
[115] L.M.B.C. Campos, On the extended hypergeometric equation and functions of arbitrary degree, *Integral Transforms and Special Functions* 11 (3) (2001) 233–256.
[116] A.R. Forsyth, *Theory of Differential Functions*, Cambridge University Press, 1902.
[117] A.R. Forsyth, *Treatise of Differential Equations*, sixth ed., MacMillan, 1926.
[118] E.T. Whittaker, G.N. Watson, *A Course of Modern Analysis*, Cambridge University Press, 1927.
[119] J.M. Miles, On the disturbed motion of a vortex sheet, *Journal of Fluid Mechanics* 4 (1958) 538–554.
[120] E.G.C. Poole, *Introduction to the Theory of Linear Differential Equations*, Oxford University Press, 1936.
[121] A.E.H. Love, *Elasticity*, Oxford University Press, 1944.